

UNIVERSITY OF PARDUBICE
JAN PERNER TRANSPORT FACULTY

BACHELOR THESIS

2009

Adam Franc

University of Pardubice
Jan Perner Transport Faculty

Use of Reinforcing Polypropylene Fibres in Soils

Adam Franc

Bachelor thesis

2009

Univerzita Pardubice
Dopravní fakulta Jana Pernera
Katedra dopravní infrastruktury
Akademický rok: 2008/2009

ZADÁNÍ BAKALÁŘSKÉ PRÁCE

(PROJEKTU, UMĚLECKÉHO DÍLA, UMĚLECKÉHO VÝKONU)

Jméno a příjmení: **Adam FRANC**

Studijní program: **B3709 Dopravní technologie a spoje**

Studijní obor: **Dopravní infrastruktura-Dopravní cesta**

Název tématu: **Použití výztužných polypropylenových vláken v zeminách**

Z á s a d y p r o v y p r a c o v á n í :

1. Zhodnocení současného stavu v řešené problematice v ČR a v zahraničí
2. Písemný elaborát provedených laboratorních zkoušek
3. Grafické a početní vyhodnocení zkoušek
4. Fotodokumentaci

Rozsah grafických prací:

Rozsah pracovní zprávy:

Forma zpracování bakalářské práce: **tištěná**

Seznam odborné literatury:

Šimek, J., Holoušová, T. Mechanika zemin a zakládání staveb Skriptum ČVUT v Praze, 1996.

Vacek, J.: Geotechnika I, UPa DFJP, Pardubice 2000.

Vacek, J.: Geotechnika II, UPa DFJP, Pardubice 2000.

Vaníček, I.: Mechanika zemin, Skripta FSV ČVUT, 2000

Hulla, J., Turček, P. Zakladanie stavieb Vyd. Jaga group, v.o.s. ISBN 80-88905-05-2, 1998.

I.Vaníček, I.Kudrnáčová, Mechanika zemin - cvičení, skriptum ČVUT

Vedoucí bakalářské práce:

Ing. Aleš Šmejda, Ph.D.

Katedra dopravní infrastruktury

Datum zadání bakalářské práce: **30. listopadu 2008**


Termín odevzdání bakalářské práce: **1. června 2009**



prof. Ing. Bohumil Culek, CSc.

děkan

L.S.



doc. Ing. Vladimír Doležel, CSc.

vedoucí katedry

dne

Prohlašuji:

Tuto práci jsem vypracoval samostatně. Veškeré literární prameny a informace, které jsem v práci využil, jsou uvedeny v seznamu použité literatury.

Byl jsem seznámen s tím, že se na moji práci vztahují práva a povinnosti vyplývající ze zákona č. 121/2000 Sb., autorský zákon, zejména se skutečností, že Univerzita Pardubice má právo na uzavření licenční smlouvy o užití této práce jako školního díla podle § 60 odst. 1 autorského zákona, a s tím, že pokud dojde k užití této práce mnou nebo bude poskytnuta licence o užití jinému subjektu, je Univerzita Pardubice oprávněna ode mne požadovat přiměřený příspěvek na úhradu nákladů, které na vytvoření díla vynaložila, a to podle okolností až do jejich skutečné výše.

Souhlasím s prezenčním zpřístupněním své práce v Univerzitní knihovně.

V Pardubicích dne 1. 6. 2009

Adam Franc

ANNOTATION

The aim of the work is to find, compare and evaluate any mechanical relationships between unreinforced clayey soil and clayey soil reinforced by randomly distributed polypropylene fibrillated fibres. The work involves the present explorations and discoveries on this problem abroad and in the Czech Republic, and compares some results of mechanical behaviour to the results found out by laboratory exams carried out within the framework of this thesis.

KEYWORDS

soil; reinforcement; polypropylene fibres; triaxial compression; deformation

NÁZEV

Použití výztužných polypropylenových vláken v zeminách

SOUHRN

Cílem této práce je najít, porovnat a zhodnotit mechanické souvislosti mezi nevyztuženou jílovitou zeminou a jílovitou zeminou vyztuženou náhodně rozmístěnými polypropylenovými fibrilovanými vlákny. Práce zahrnuje dosavadní průzkumy a objevy v této oblasti doma i v zahraničí a porovnává některé výsledky chování zeminy s výsledky zjištěnými laboratorními zkouškami v rámci této bakalářské práce.

KLÍČOVÁ SLOVA

zemina; vyztužení; polypropylenová vlákna; triaxiální tlak; přetvoření

Acknowledgements

Many thanks belong to all authors providing free material on the internet, as well as to those who let their papers be viewed.

Warm thanks belong to my family for its patience and support when my work made me busy and I often couldn't take part in housekeeping.

Finally and especially, I want to thank Ing. Aleš Šmejda, Ph.D., my supervisor, for his readily help and great, friendly attitude, which had principal effect on successful accomplishment of my work. Mr Šmejda ,thank you very much indeed.

CONTENTS

List of Figures	7
PART ONE: Background literature review, geotechnical terms & issues	12
1. Introduction	13
2. Geosynthetics	14
2.1. <i>Related Terms</i>	14
2.2. <i>Definitions and Types</i>	14
2.3. <i>Manufacture</i>	16
2.4. <i>Functions and Applications</i>	16
2.5. <i>Geosynthetics for Soil Reinforcement</i>	17
2.6. <i>Polypropylene Fibrillated Fibres</i>	17
2.6.1. <i>Method</i>	17
2.6.2. <i>Existing Studies</i>	18
2.6.3. <i>Potential Applications</i>	19
2.7. <i>Use of Micro-reinforcement Polypropylene Fibres in the Czech Republic</i>	21
2.8. <i>Conclusion</i>	21
3. Soil Classification	21
3.1. <i>Objective</i>	21
3.2. <i>Method</i>	21
3.2.1. <i>Laboratory Examinations – Description</i>	22
3.2.2. <i>Visual Examination</i>	25
4. Laboratory Tests	27
4.1. <i>Particle Size Distribution (Grain Size Distribution)</i>	27
4.1.1. <i>Sieve Analysis</i>	27
4.1.2. <i>Sedimentation Technique (Hydrometer Analysis)</i>	29
4.2. <i>Atterberg Limits</i>	30
4.2.1. <i>Shrinkage Limit</i>	30
4.2.2. <i>Plastic Limit</i>	30
4.2.3. <i>Liquid Limit</i>	30
4.2.4. <i>Derived limits</i>	32
4.3. <i>Other Commonly Determinated Soil Properties</i>	33
4.3.1. <i>Bulk density</i>	33
4.3.2. <i>Specific weight</i>	33
4.3.3. <i>Wetness</i>	33

4.4.	<i>Maximum Bulk Density</i>	34
4.5.	<i>Pure Compression (Unconfined Compression)</i>	35
4.6.	<i>Undrained Triaxial Test</i>	37
PART TWO: Laboratory Research soil & fibre material, characterisations and tests		41
5.	Laboratory Instrumentation	42
6.	Specimen Laboratory Testings	44
6.1.	<i>Soil Specimen Elementary Characterisation</i>	44
6.2.	<i>Standard Proctor Test</i>	46
6.3.	<i>Pycnometer Test (Specific Weight)</i>	46
6.4.	<i>Grain Size Analysis</i>	47
6.5.	<i>Specimen Classification</i>	50
6.6.	<i>Pure Compression</i>	50
6.7.	<i>Triaxial Compression</i>	53
6.7.1.	Unreinforced Soil Testing.....	53
6.7.2.	Reinforced Soil Testing	55
6.7.2.1.	Test I. 0.5% Reinforcement.....	57
6.7.2.2.	Test III. 1% Reinforcement	61
6.7.2.3.	Evaluation by Mohr's Circle Diagram	64
7.	Conclusion	66
Bibliography		67

LIST OF FIGURES

<i>Figure 2-1. Geotextile [13]</i>	14
<i>Figure 2-2. Geogrid[14]</i>	14
<i>Figure 2-3. Geonet[15]</i>	14
<i>Figure 2-4. Classification of geosynthetics and other soil inclusions [1]</i>	15
<i>Figure 2-5. Polypropylene fibres „Geofibers“ by Synthetic Industries (USA) [4]</i>	18
<i>Figure 2-6. Fibre „Texsol“ by Kordárna a.s. (Czech Republic), employed in the thesis [0]</i>	19
<i>Figure 3-1. Sieve numbers [12]</i>	22
<i>Figure 3-2. Unified Soil Classification System – ASTM D2488 [11]</i>	23
<i>Figure 3-3. Letter symbols for soil divisions [5]</i>	24
<i>Figure 3-4. Plasticity Chart for the Unified Soil Classification System [10]</i>	24
<i>Figure 3-5. Soil classification diagram ČSN ISO 14688-2 [25]</i>	26
<i>Figure 4-1. Principle of sifting [6]</i>	28

Figure 4-2. Apparatus and stack of sieves for grain size distribution test [0]	28
Figure 4-3. Progress of particles sedimentation, performed on the thesis' sample [0]	29
Figure 4-4. 3 mm diameter threads, test of plasticity on the thesis' sample [0]	30
Figure 4-5. Cone penetrometer – apparatus for measuring the cone penetration [9]	31
Figure 4-6. Cone standardised geometry and mass [9]	32
Figure 4-7. Pycnometer with boiling suspension in a sand bath [0].....	33
Figure 4-8. The Proctor mortar and rammer [0].....	34
Figure 4-9. Bulk density – moisture relationship, the Proctor test.....	35
Figure 4-10. Mould for remoulded specimen preparation [0].....	36
Figure 4-11. Stress-strain curve of a metal (Stress, kPa; strain, %) [18].....	37
Figure 4-12. Shear breaking plane, unconfined compression test of the thesis' sample [0].....	37
Figure 4-13. Specimen prepared for triaxial test [0].....	39
Figure 4-14. Triaxial running the thesis' soil specimen [0].....	39
Figure 4-15. The Mohr circle [19].....	40
Figure 4-16. Evaluation of the triaxial test [19]	40
Figure 5-1. Triaxial ELE Multiplex 50 [0].....	42
Figure 5-2. Kern 600-2M [21]	43
Figure 5-3. Balance Kern DE60K20 [0].....	43
Figure 5-4. Oven Venticell 111 [0]	44
Figure 6-1. Determination of specimen density and wetness	44
Figure 6-2. Data for determining liquidity limit.....	45
Figure 6-3. Regressive curve for obtaining the liquidity limit.....	45
Figure 6-4. Plastic limit data	45
Figure 6-5. Standard Proctor test data	46
Figure 6-6. Regressive curve for determining the optimal wetness.....	46
Figure 6-7. Specific weight, measured data	46
Figure 6-8. Temperature correction chart [7]	47
Figure 6-9. Dynamic viscosity according to temperature [7]	48
Figure 6-10. Dynamic viscosity – temperature relationship according to the table above.....	48
Figure 6-11. Sedimentation technique, input data	48
Figure 6-12. Hydrometer test, data measured and computed	49
Figure 6-13. Grain size curve of the thesis' soil sample	49
Figure 6-14. Calibration chart for the measuring ring	51
Figure 6-15. Calibration curve for the measuring ring.....	51
Figure 6-16. Pure compression test, data measured and computed.....	52
Figure 6-17. Pure compression test, stress-deformation curves	53
Figure 6-18. Triaxial test of unreinforced soil, data measured and computed	54
Figure 6-19. Triaxial test of unreinforced soil, stress-deformation curves	55
Figure 6-20. Widht extension of the fibres [24]	55
Figure 6-21. Mechanical property of the Texusol fibres [24]	56

<i>Figure 6-22. Mixture of soil and fibres [0]</i>	56
<i>Figure 6-23. Triaxial test of 0.5% reinforced soil I, data measured and computed</i>	58
<i>Figure 6-24. Triaxial test of 0.5% reinforced soil, stress-deformation curves</i>	58
<i>Figure 6-25. Reinforced specimens after triaxial test (1) unconfined (2) confined compression [0]</i>	59
<i>Figure 6-26. Shear breaking plane, reinforced specimen [0]</i>	59
<i>Figure 6-27. Triaxial test of 0.5% reinforced soil II, data measured and computed</i>	60
<i>Figure 6-28. Stress-deformation curves of reinforced and unreinforced triaxial-tested samples</i>	61
<i>Figure 6-29. Triaxial test of 1% reinforced soil, data measured and computed</i>	63
<i>Figure 6-30. Stress-deformation curves, Test III (1% reinforcement) + unreinforced specimens</i>	63
<i>Figure 6-31. Stress-Strain Curves for Clay [3]</i>	64
<i>Figure 6-32. Stress-Strain Curves for Sand [3]</i>	64

PART ONE: Background

literature review, geotechnical terms & issues

1. Introduction

The use of inclusions to improve the mechanical properties of soils dates to ancient times. However, it is only within the last quarter of century or so that analytical and experimental studies have led to the contemporary soil reinforcement techniques. [2]

Soil reinforcement is now a highly attractive alternative for embankment and retaining wall projects because of the economic benefits it offers in relation to conventional retaining structures. Moreover, its acceptance has also been triggered by a number of technical factors, that include aesthetics, reliability, simple construction techniques, good seismic performance, and the ability to tolerate large deformations without structural distress. [2] This technology is also very useful in terms of modern industrial world approach, which has introduced terms such as *environment-friendly*, *sustainable development*, etc.

One of the most recent technologies discovered in the sphere of soil reinforcement is micro-reinforcement by short thin plastic fibres. In this method, the fibres are evenly mixed in the soil, in situ. The soil is then compacted layer by layer, as in usual procedures of ground improvement. The fibres-reinforced soil is to have, reportedly, higher bearing capacity and slower, gradual settlement. The thesis' conclusion should match this statement.

First, the issues of soil and soil reinforcement needs to be introduced.

2. Geosynthetics

2.1. Related Terms

Ground improvement or *ground modification* engineering is the collective term for any mechanical, hydrological, physicochemical, biological methods or any combination of such methods employed to improve certain properties of natural or man-made soil deposits.

The term *reinforced soil* refers to a soil strengthened by a material capable of resisting tensile stresses and interacting with the soil through friction and/or adhesion.

A *geosynthetic* is defined as a planar product manufactured from a polymeric material used with soil, rock, earth, or other geotechnical-related material as an integral part of a civil engineering project, structure, or system. [1]

2.2. Definitions and Types

A *geotextile* (Figure 2-1) is a permeable geosynthetic made of textile materials. *Geogrids* (Figure 2-2) are primarily used for reinforcement; they are formed by a regular network of tensile elements with apertures of sufficient size to interlock with surrounding fill material. *Geonets* (Figure 2-3) are formed by the continuous extrusion of polymeric ribs at acute angles to each other. They have large openings in a netlike configuration and the primary function of geonets is drainage. *Geomembranes* are low permeability geosynthetics used as fluid barriers. Geotextiles and related products such as nets and grids can be combined with geomembranes and other synthetics to take advantage of the best attributes of each component. These products are called *geocomposites*, and they may be composites of geotextile-geonets, geotextile-geogrids, geotextile-geomembranes, geomembrane-geonets, geotextile-polymeric cores, and even threedimensional polymeric cell structures. There is almost no limit to the variety of geocomposites that are possible and useful. The general generic term encompassing all these materials is *geosynthetic*. A convenient classification system for geosynthetics is given in Figure 2-4. [1]



Figure 2-1. Geotextile [13]



Figure 2-2. Geogrid [14]



Figure 2-3. Geonet [15]

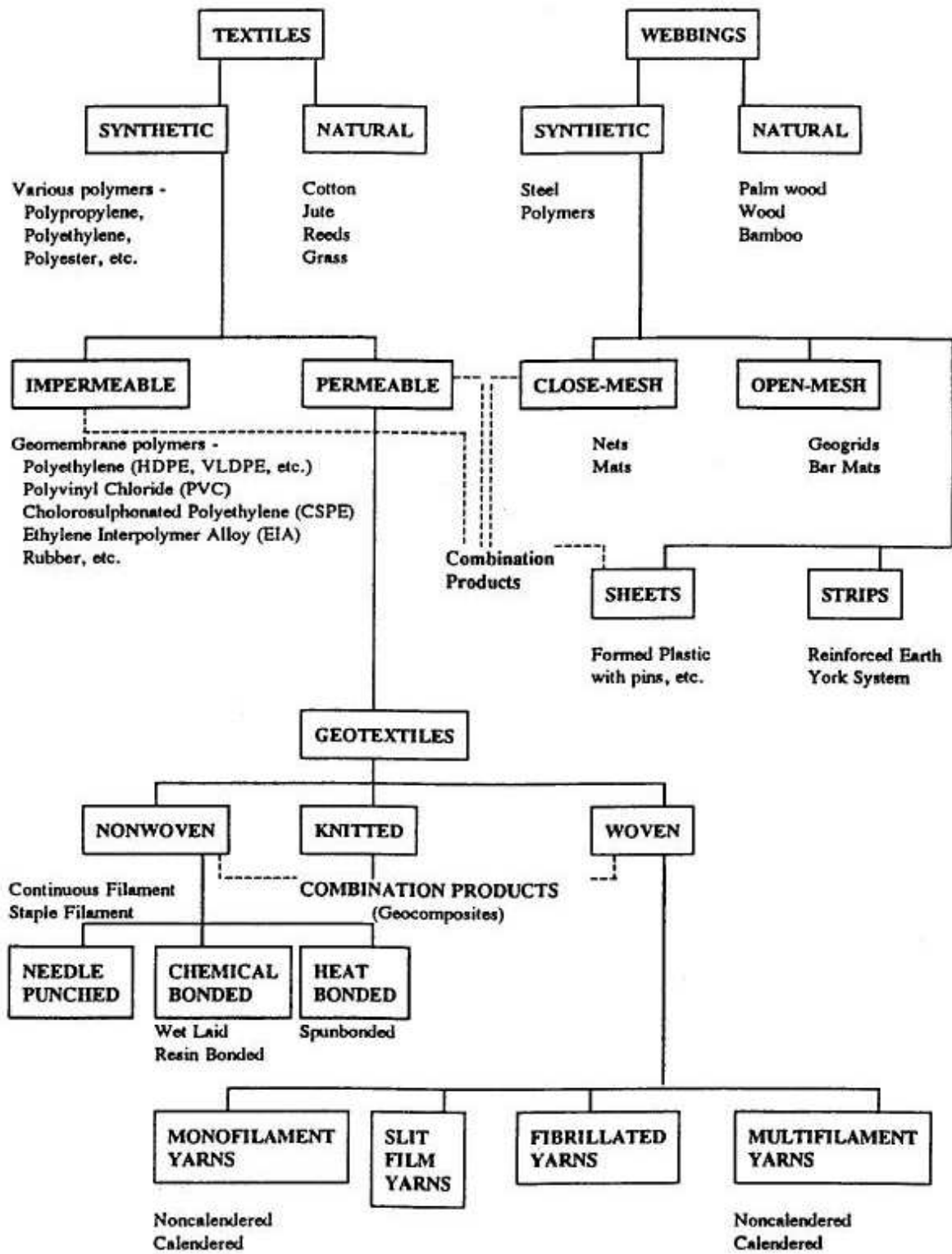


Figure 2-4. Classification of geosynthetics and other soil inclusions [1]

2.3. Manufacture

Most geosynthetics are made from synthetic polymers such as polypropylene, polyester, polyethylene, polyamide, PVC, etc. These materials are highly resistant to biological and chemical degradation.

In manufacturing geotextiles, elements such as fibres or yarns are combined into planar textile structures. The fibres can be continuous *filaments*, which are very long thin strands of a polymer, or *staple fibres*, which are short filaments, typically 20 to 100 mm long. The fibres may also be produced by slitting an extruded plastic sheet or film to form thin flat tapes. In both filaments and slit films, the extrusion or drawing process elongates the polymers in the direction of the draw and increases the fibre strength.

Geotextile type is determined by the method used to combine the filaments or tapes into the planar textile structure. The vast majority of geotextiles are either *woven* or *nonwoven*. Woven geotextiles are made of *monofilament*, *multifilament*, or *fibrillated* yarns, or of slit films and tapes. Although the weaving process is very old, nonwoven textile manufacture is a modern industrial development. Synthetic polymer fibers or filaments are continuously extruded and spun, blown or otherwise laid onto a moving belt. Then the mass of filaments or fibers are either *needlepunched*, in which the filaments are mechanically entangled by a series of small needles, or *heat bonded*, in which the fibers are *welded* together by heat and/or pressure at their points of contact in the nonwoven mass.

Stiff geogrids with integral junctions are manufactured by extruding and orienting sheets of polyolefins. Flexible geogrids are made of polyester yarns joined at the crossover points by knitting or weaving, and coated with a polymer. [1]

2.4. Functions and Applications

Geosynthetics have six primary functions:

1. filtration,
2. drainage,
3. separation,
4. reinforcement,
5. fluid barrier,
6. protection.

Geosynthetic applications are usually defined by their primary, or principal function. In a number of applications, in addition to the primary function, geosynthetics usually perform one or

more secondary functions. It is important to consider both the primary and secondary functions in the design computations and specifications. [1]

2.5. Geosynthetics for Soil Reinforcement

The three primary applications soil reinforcement using geosynthetics are

1. reinforcing the base of embankments constructed on very soft foundations,
2. increasing the stability and steepness of slopes,
3. reducing the earth pressures behind retaining walls and abutments.

In the first two applications, geosynthetics permit construction that otherwise would be cost prohibitive or technically not feasible. In the case of retaining walls, significant cost savings are possible in comparison with conventional retaining wall construction. Other reinforcement and stabilization applications in which geosynthetics have also proven to be very effective include roads and railroads, large area stabilization, and natural slope reinforcement. [1]

2.6. Polypropylene Fibrillated Fibres

2.6.1. Method

Traditional methods of soil reinforcement involve the use of continuous planar inclusions (e.g. metallic strips, geogrids, geotextiles) within earth structures. The inclusions provide tensile resistance to the soil in a particular direction. Planes of weakness may be introduced along the interface between reinforcement and soil. Short discrete fibers, if mixed uniformly within the soil mass, can provide isotropic increase in the strength of the soil composite without introducing continuous planes of weakness. Also, fiber-reinforcement solutions do not require design considerations regarding anchorage as planar reinforcements do. The technique of fiber-reinforcement has been increasingly adopted in geotechnical projects involving repair of failed slope and stabilization of thin soil veneers. [4]



Figure 2-5. Polypropylene fibres „Geofibers“ by Synthetic Industries (USA) [4]

2.6.2. Existing Studies

Synthetic fibers have been used since the late 1980s, when the initial studies using polymeric fibers were conducted. Specifically, triaxial compression tests, unconfined compression tests, and direct shear tests have been conducted to study the effect of fiber-reinforcement on shear strength. Previous research has shown that **fiber-reinforcement can significantly increase the peak shear strength and limit the post-peak shear strength loss of a soil mass.**

Most of the experimental studies were conducted using granular soils. Gray and Ohashi (1983) studied the mechanisms of fiber-reinforcement using direct shear tests. Fibers were placed at different specific orientations with respect to the shear plane. The fiber content, orientation of fibers, and modulus of fibers were found to influence the contribution of fibers to the shear strength. Al-Refeai (1990) studied the effect of fiber-reinforcement using different types of granular soils and fibers. The effect of fiber-reinforcement was found to be more significant in fine sand with subrounded particles than in medium grained sand with subangular particles. The extensibility of the fibers was also found to influence the soil-fiber interaction.

Research on the use of fiber-reinforcement with cohesive soils has been more limited. Although fiber-reinforcement was reported to increase the shear strength of cohesive soils, such improvement needs additional evaluation because the load transfer mechanisms on the interface between fibers and clayey soils are not clearly understood. Andersland and Khattack (1979) performed tests on kaolinite clay reinforced with cellulose pulp fibers. The shear strength under various testing conditions (undrained, consolidated drained, and consolidated undrained) increased with increasing fiber content. The ductility of the specimen was also found to increase with increasing fiber content. The load transfer mechanism on the fiber-soil interface was explained as

an attraction between soil particles and fibers. Maher and Ho (1994) reported that randomly distributed fibers increase the peak unconfined compressive strength, ductility, splitting tensile strength and flexural toughness of kaolinite clay. The contribution of fiber-reinforcement was found to be more significant for specimens with lower water contents.

While significant research has been conducted so far on the analysis and design of structures with continuous planar reinforcement, the behavior of soils reinforced with randomly distributed fibers needs additional evaluation. Past research has shown that the addition of fibers within soil increases the peak shear strength and reduces the post-peak strength loss. [4]

2.6.3. Potential Applications

Fiber-reinforcement has been considered in projects involving

- slope stabilization,
- embankment construction,
- subgrade stabilization,
- stabilization of thin veneers such as landfill covers.

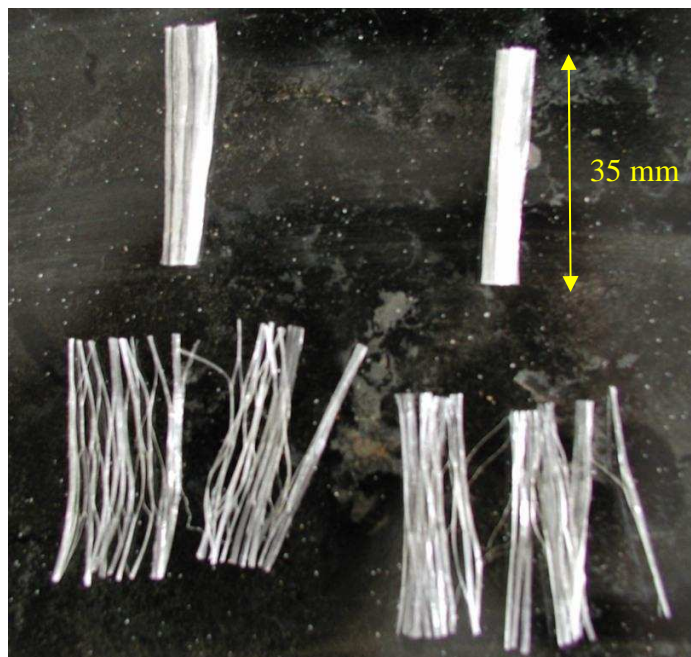


Figure 2-6. Fibre „Texsol“ by Kordárna a.s. (Czech Republic), employed in the thesis [0]

The general advantages of fiber-reinforcement are:

(1) Field placement of fibers can be done using conventional construction equipment. A rotary mixer of the type typically used in lime-soil mixing can be used to mix the fibers within the soil lift. The lift can then be compacted using standard soil compaction methods, without the concern of damaging the reinforcement.

(2) Unlike lime, cement and other chemical stabilization methods, the construction using fiber-reinforcement is not significantly affected by weather conditions.

(3) The materials that can be used for fiber-reinforcement are widely available. Plant roots, shredded tires, and recycled waste fibers can also be used as reinforcement in addition to factory-manufactured synthetic fibers.

A promising application of fiber-reinforcement is in the localized repair of failed slopes. In this case, the irregular shape of the soil “patches” limits the use of continuous planar reinforcement, making the fiber-reinforcement an appealing alternative. Unlike planar reinforcement, fiber-reinforcement does not require a large anchorage length, thus minimizing the excavation depth.

Another application is the stabilization of soil veneers (e.g. landfill covers) that are too steep for stabilization using parallel-to-slope continuous reinforcements (Zornberg et al., 2001; Zornberg, 2005). Continuous horizontal reinforcement has been used, but this requires anchoring of the reinforcement into competent material underlying the soil veneer. Also, parallel-to-slope reinforcement requires anchoring the reinforcement at the slope crest. In contrast, the use of discrete fibers does not require anchoring, and is economically and technically feasible.

In pavement construction, fiber-reinforcement can be used to stabilize a wide variety of subgrade soils ranging from sand to high-plasticity clays (Santoni, et al., 2001; Grogan and Johnson, 1993). The number of passes to failure in field road test was reported to increase by fiber-reinforcement.

Fiber-reinforcement has also been used in combination with planar geosynthetics for reinforced slopes or walls (Gregory, 1998). By increasing the shear strength of the backfill materials, fiber reinforcement reduces the required amount of planar reinforcement and may eliminate the need for secondary reinforcement. Fiber-reinforcement has been reported to be helpful in eliminating the shallow failure on the slope face and reducing the cost of maintenance.

Fibers have also been reported to provide cracking control (Ziegler et al., 1998; Allan and Kukacka, 1995). Earth structures constructed using clayey soils develop desiccation cracks when subjected to wet-dry cycles. Fibers were found to effectively reduce the number and width of desiccation cracks. Fiber reinforcement can also mitigate potential cracking induced by differential settlements because fiber-reinforcement increases the ductility of the soil.

Fiber-reinforcement can also provide erosion control and facilitate vegetation development since the compaction effort needed for fiber-reinforced soil is less than for unreinforced soil of equivalent strength.

Fiber-reinforcement has also been used for stabilization of expansive soil (Puppala, 2000).

Fibers were found to reduce shrinkage and swell pressures of expansive clays.

The inclusion of fibers was also reported to improve the response of a soil mass subjected to dynamic loading (Maher and Woods, 1990; Noorany and Uzdavines, 1989). [4]

2.7. Use of Micro-reinforcement Polypropylene Fibres in the Czech Republic

Although the geosynthetics market and its product range in the Czech Republic is relatively rich, no great mark of use occurs. The range of macro-reinforcement geosynthetics – geotextiles, geogrids, geonets etc probably involves all the world-widely used elementary geosynthetics products and methods.

There are some companies which produce geosynthetics for micro-reinforcement or work on its research, namely Kordárna, a.s., of which fibres (Texsol) are employed for the research in this thesis. Nevertheless, these geosynthetics still haven't been evaluated enough to become a part of the market with geosynthetics.

Phenomenon of the micro-reinforcement is at the beginning phase both in the world and the Czech Republic, although there are considerably more studies researching the matter abroad (especially in U. S. A.).

2.8. Conclusion

In less than 30 years, geosynthetics have revolutionized many aspects of our practice, and in some applications they have entirely replaced the traditional construction material. In many cases, the use of a geosynthetic can significantly increase the safety factor, improve performance, reduce impact on environment, and reduce costs in comparison with conventional design and construction alternatives. [1] However, reinforced soil with randomly distributed fibres as one of the reinforcing techniques hasn't been explored and evaluated enough, although it could have principal effect on existing geotechnical engineering know-how.

3. Soil Classification

3.1. Objective

The principal objective of soil classification is the **prediction of engineering properties and behavior of a soil** based on a few simple laboratory or field tests. The results of these tests are then used to identify the soil and put it into a group of soils that have similar engineering characteristics. [5] An important part of soil classification is **the particle size distribution** and the *Atterberg limits* [6] (more in chapter 4: Laboratory Tests).

3.2. Method

Geotechnical engineering recognizes several systems of soil classification, e. g. the most widely used systems in the United States are USCS (**Unified Soil Classification System**) –

internationally recognized system, AASHTO (American Association of State Highway and Transportation Officials) Soil Classification System, Inorganic Soil Classification System – based on plasticity, USDA (U. S. Department of Agriculture) Textural Soil Classification System, etc. (more information in [6]). Classification system used in the Czech Republic is defined by a Czech norm ČSN ISO 14688-2 (classification diagram p. 26).

Soils seldom exist in nature separately as sand, gravel, or any other single component. Soils usually form mixtures with varying proportions of different size particles. Each component contributes to the characteristics of the mixture. The USCS is based on the textural or plasticity-compressibility characteristics that indicate how a soil will behave as a construction material. In the USCS, all soils are divided into **three major divisions**:

- (1) coarse grained, (2) fine grained, and (3) highly organic.

3.2.1. Laboratory Examinations – Description

Coarse-grained and fine-grained soils are distinguished by the amount of material that is either retained on or that passes a No. 200 sieve (Figure 3-1). If 50 percent or more of the soil by weight is retained on a No. 200 sieve, then the soil is coarse-grained. It is fine-grained if more than 50 percent passes the No. 200 sieve. Highly organic soils can generally be identified by visual examination. The major divisions are further subdivided into soil groups. The USCS uses 15 groups and each group is distinguished by a descriptive name and letter symbol, as shown in Figure 3-2. [5]

Sieve Number	Opening Size (mm)
4	4.750
6	3.350
8	2.360
12	1.680
16	1.180
20	0.850
30	0.600
40	0.425
50	0.300
60	0.250
80	0.180
100	0.150
140	0.106
200	0.075
270	0.053

Figure 3-1. Sieve numbers [12]

MAJOR DIVISION		GROUP SYMBOL	LETTER SYMBOL	GROUP NAME	
COARSE GRAINED SOILS CONTAINS MORE THAN 50% FINES	GRAVEL AND GRAVELLY SOILS MORE THAN 50% OF COARSE FRACTION RETAINED ON NO. 4 SIEVE	GRAVEL WITH *5% FINES		GW	Well-graded GRAVEL
				GP	Poorly graded GRAVEL
		GRAVEL WITH BETWEEN 5% AND 15% FINES		GW-GM	Well-graded GRAVEL with silt
				GW-GC	Well-graded GRAVEL with clay
				GP-GM	Poorly graded GRAVEL with silt
				GP-GC	Poorly graded GRAVEL with clay
	GRAVEL WITH ≥ 15% FINES		GM	Silty GRAVEL	
			GC	Clayey GRAVEL	
	SAND AND SANDY SOILS MORE THAN 50% OF COARSE FRACTION PASSING ON NO. 4 SIEVE	SAND WITH *5% FINES		SW	Well-graded SAND
				SP	Poorly graded SAND
		SAND WITH BETWEEN 5% AND 15% FINES		SW-SM	Well-graded SAND with silt
				SW-SC	Well-graded SAND with clay
				SP-SM	Poorly graded SAND with silt
				SP-SC	Poorly graded SAND with clay
		SAND WITH ≥ 15% FINES		SM	Silty SAND
			SC	Clayey SAND	
FINE GRAINED SOILS CONTAINS MORE THAN 50% FINES	SILT AND CLAY	LIQUID LIMIT LESS THAN 50		ML	Inorganic SILT with low plasticity
				CL	Lean inorganic CLAY with low plasticity
				OL	Organic SILT with low plasticity
	LIQUID LIMIT GREATER THAN 50		MH	Elastic inorganic SILT with moderate to high plasticity	
			CH	Fat inorganic CLAY with moderate to high plasticity	
			OH	Organic SILT or CLAY with moderate to high plasticity	
HIGHLY ORGANIC SOILS			PT	PEAT soils with high organic contents	

Figure 3-2. Unified Soil Classification System – ASTM D2488 [11]

NOTES:

- 1) Sample descriptions are based on visual field and laboratory observations using classification methods of ASTM D2488. Where laboratory data are available, classifications are in accordance with ASTM D2487.
- 2) Solid lines between soil descriptions indicate change in interpreted geologic unit. Dashed lines indicate stratigraphic change within the unit.
- 3) Fines are material passing the U.S. Std. #200 Sieve.

The letter symbols are derived either from the terms descriptive of the soil fractions, the relative value of the liquid limit (high or low), or the relative gradation of the soil (well graded or poorly graded). The letters that are used in combination to form the 15 soil groups are as follows:

SOIL TYPE	GRADATION	LIQUID LIMIT (LL)
Gravel—G	Well graded—W	LL over 50—H
Sand—S	Poorly graded—P	LL under 50—L
Silt—M		
Clay—C		
Organic—O		
Peat—Pt		

Figure 3-3. Letter symbols for soil divisions [5]

As the soil sample being investigated in this thesis (hereinafter „thesis‘ sample“) belongs to the fine-grained soils, the following text will focus on this group only.

Fine-grained soils

The fine-grained soils are not classified on the basis of grain size distribution, but according to plasticity and compressibility. Laboratory classification criteria are based on the relationship between the liquid limit and plasticity index as designated in the *plasticity chart* in Figure 3-4. This chart was established by the determination of limits for many soils, together with an analysis of the effect of limits upon physical characteristics. Examination of the chart shows that there are two major groupings of fine-grained soils. These are the L groups, which have liquid limits less than 50, and the H groups, which have liquid limits equal to and greater than 50. The symbols L and H have general meanings of low and high compressibility, respectively. Fine-grained soils are further divided with relation to their position above or below the A-line of the plasticity chart. [5]

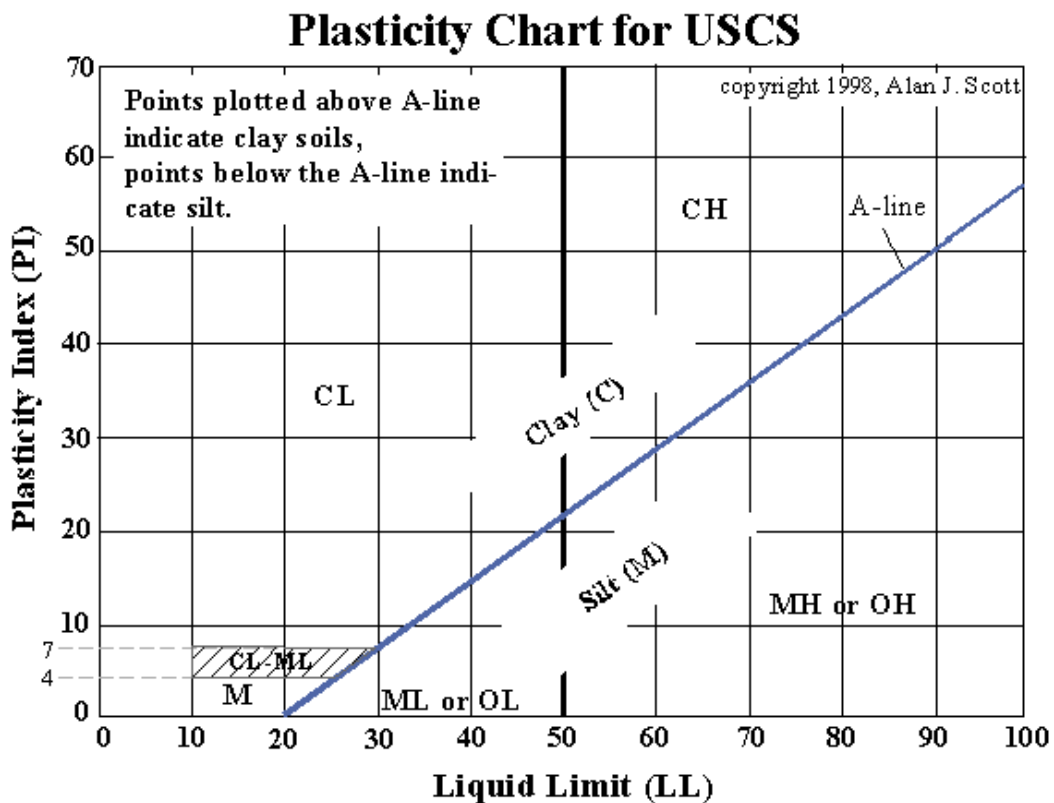


Figure 3-4. Plasticity Chart for the Unified Soil Classification System [10]

ML and MH Groups

Typical soils of the ML and MH groups are inorganic silts. Those of low compressibility are in the ML group. Others are in the MH group. All of these soils plot below the A-line of the plasticity chart. The ML group includes very fine sands, rock flours (rock dust), and silty or clayey fine sand or clayey silts with low plasticity. Loess type soils usually fall into this group. Diatomaceous and micaceous soils usually fall into the MH group but may fall into the ML group when the liquid limit is less than 50. Plastic silts fall into the MH group.

CL and CH Groups

In these groups, the symbol C stands for clay, with L and H denoting low or high liquid limits. These soils plot above the A-line and are principally inorganic clays. In the CL group are included gravelly clays, sandy clays, silty clays, and lean clays. In the CH group are inorganic clays of high plasticity.

OL and OH Groups

The soils in these two groups are characterized by the presence of organic matter; hence the symbol O. All of these soils generally plot below the A-line. Organic silts and organic silt-clays of high plasticity fall into the OL group, while organic clays of high plasticity plot in the OH zone of the plasticity chart. Many of the organic silts, silt-clays, and clays deposited by the rivers along the lower reaches of the Atlantic seaboard have liquid limits above 40 and plot below the A-line. Peaty soils may have liquid limits of several hundred percent and plot well below the A-line because of their high percentage of decomposed vegetational matter. A liquid limit test, however, is not a true indicator in cases in which a considerable portion consists of other than soil matter. [5]

3.2.2. Visual Examination

Visual examination should establish the color, grain size, grain shapes (of the coarse-grained portion), some idea of the gradation, and some properties of the undisturbed soil. Color is often helpful in distinguishing between soil types, and with experience, one may find it useful in identifying the particular soil type. Color may also indicate the presence of certain chemicals. Color often varies with moisture content of a soil. For this reason, the moisture content at the time of color identification should be included.

Familiar color properties (selected principal ones for the thesis' sample):

- Generally, colors become darker as the moisture content increases and lighter as the soil dries.
- Some fine-grained soils (OL, OH) with dark drab shades of brown or gray, including almost black, contain organic colloidal matter.
- In contrast, clean, bright looking shades of gray, olive green, brown, red, yellow, and white are associated with inorganic soils. [5]

Czech norm ČSN ISO 14688-2 uses for the purpose of soil classification the following diagram:

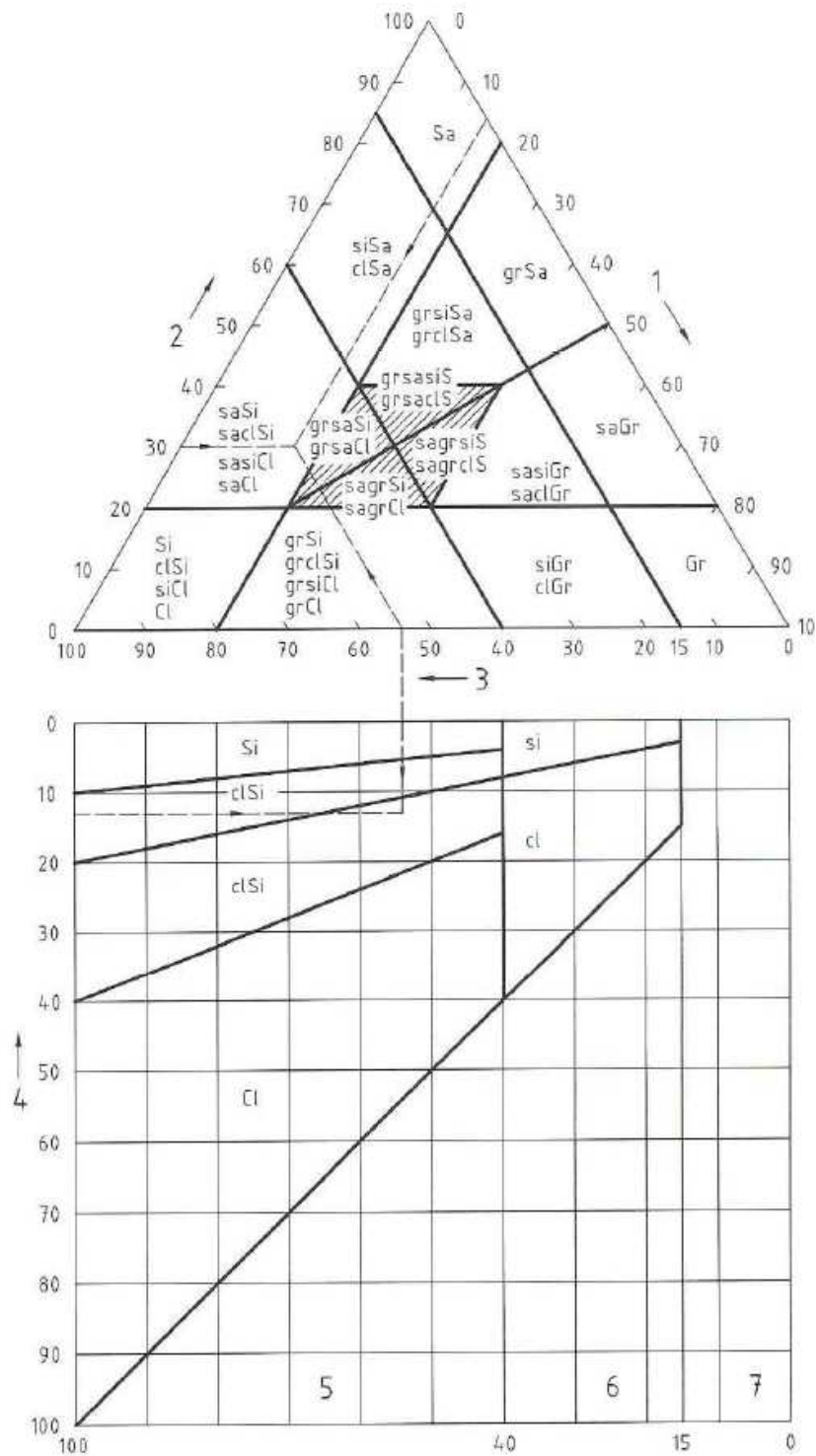


Figure 3-5. Soil classification diagram ČSN ISO 14688-2 [25]

4. Laboratory Tests

Soil can be examined by many methods and procedures, depending on the information, parameters of the soil, that we need to obtain. First, if the soil is to be identified, its elementary properties must be determined. Only a few basic tests need to be performed in order to classify a soil sample, as mentioned in chapter 3: Soil Classification:

- particle size distribution,
- Atterberg limits,
 - liquid limit,
 - plastic limit,
 - shrinkage limit.

4.1. Particle Size Distribution (Grain Size Distribution)

There are two procedures based on the grains sizes. The sieve analysis distributes grains of sizes larger than 0.063 mm in diameter. Distribution of the grains smaller than 0.063 in diameter can be researched by the sedimentation technique.

4.1.1. Sieve Analysis

This test is performed by a set of sieves laid in size order one on another in a stack. The top sieve has the largest openings, the bottom one has the smallest openings. The investigated soil material first undergoes preparation procedures – air-drying, dividing soil pieces stuck together (without crushing the fundamental grains!), then is weighed and put on the uppermost sieve. The stack of sieves is then placed and fastened to a vibrating apparatus, covered, and shaken for a specified time.

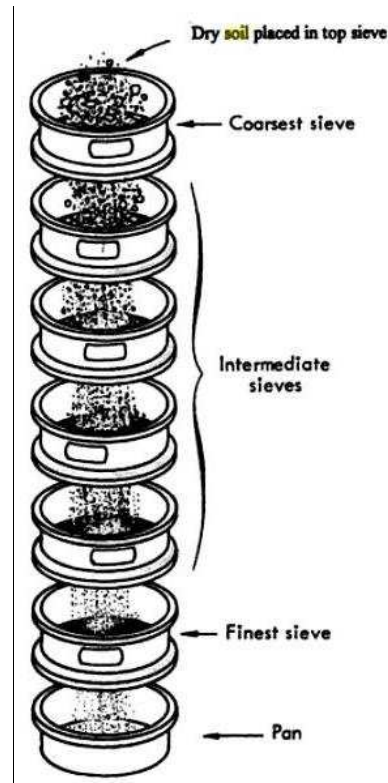


Figure 4-1. Principle of sifting [6]

Afterwards, the separated sieves residues are weighed and expressed as the mass percentual fragments.

If the finest sieve residue (0.063 mm) exceeds 10% of the entire soil mass, it is explored further by the sedimentation technique. [7]



Figure 4-2. Apparatus and stack of sieves for grain size distribution test [0]

4.1.2. Sedimentation Technique (Hydrometer Analysis)

It is employed to identify percentual portions of very fine fractions (particle size less than 0,063 mm in diameter) of a soil. This method is based on the Stokes Law, which defines a certain mathematical relationship between a particle size and its speed of sinking (under certain ideal circumstances) in water. [7] Particle sinking and measuring of the suspension density is carried out in a 1000 ml glass graduated cylinder filled to the top. Figure 4-3 documents the test. Input data for the test conclusions are:

- values read from the hydrometer gauge collected at certain time intervals,
- calibration equation or chart for the hydrometer gauge reading,
- temperature of the liquid measured at certain time intervals,
- amount of the fluid (1000 ml),
- amount of the soil,
- specific weight of the soil (4.3.2).

After test processing and evaluation (2nd part of the thesis), the fine soil part of the *grain size curve* can be constructed. Together with the previously described sieve analysis, the grain size curve is complete, and we have the result of the grain size distribution test – knowledge of the exact mass portions of the single soil fractions.

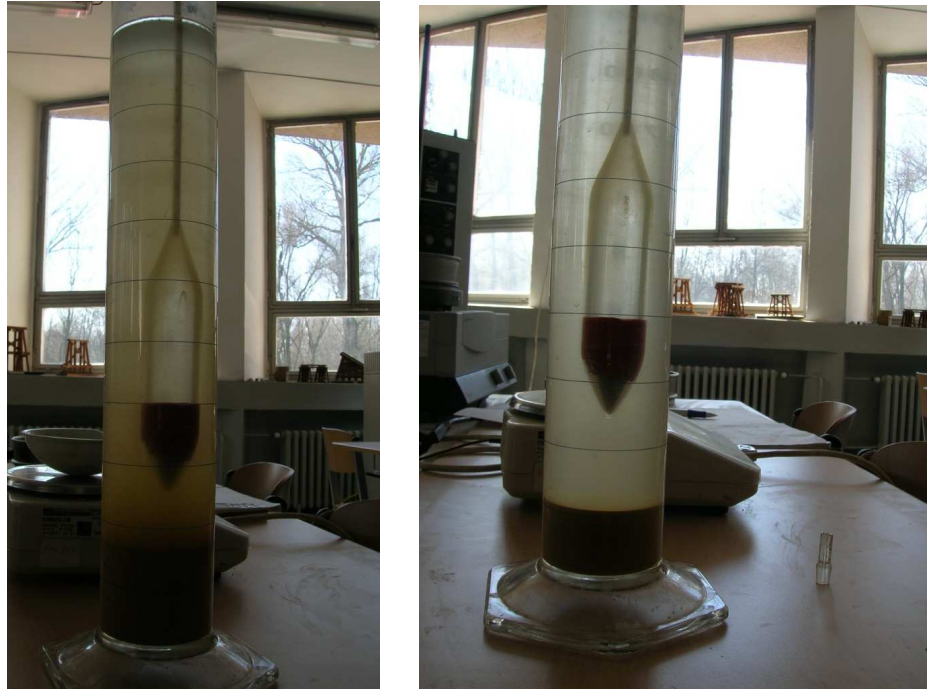


Figure 4-3. Progress of particles sedimentation, performed on the thesis' sample [0]

4.2. Atterberg Limits

The Atterberg limits are a basic measure of the nature of a fine-grained soil. Depending on the water content of the soil, it may appear in four states: *solid*, *semi-solid*, *plastic* and *liquid*. In each state the consistency and behavior of a soil is different and thus so are its engineering properties. Thus, the boundary between each state can be defined based on a change in the soil's behavior. The Atterberg limits can be used to distinguish between silt and clay. [8]

4.2.1. Shrinkage Limit

The shrinkage limit is the water content where further loss of moisture will not result in any more volume reduction. The test to determine the shrinkage limit is ASTM International D427. The shrinkage limit is much less commonly used than the liquid limit and the plastic limit.

The shrinkage limit is not utilized in this thesis.

4.2.2. Plastic Limit

The plastic limit w_p is the water content where soil starts to exhibit plastic behavior. A thread of soil is at its plastic limit when it is rolled to a diameter of 3 mm or begins to crumble (Figure 4-4). To improve consistency, a 3 mm diameter rod is often used to gauge the thickness of the thread when conducting the test.



Figure 4-4. 3 mm diameter threads, test of plasticity on the thesis' sample [0]

4.2.3. Liquid Limit

The liquid limit w_L is the water content where a soil changes from plastic to liquid behavior.

Casagrande's method

Soil is placed into the metal cup portion of the device and a groove is made down its center with a standardized tool. The cup is repeatedly dropped 10 mm onto a hard rubber base during which the groove closes up gradually as a result of the impact. The number of blows for the groove to close for 13 mm is recorded. The moisture content at which it takes 25 drops of the cup to cause the groove to close is defined as the liquid limit.

Cone penetrometer method

Another method for measuring the liquid limit is the cone penetrometer test. It is based on the measurement of penetration into the soil of a standardized cone of specific mass. Despite the universal prevalence of the Casagrande method, the cone penetrometer is often considered to be a more consistent alternative because it minimizes the possibility of human variations when carrying out the test.

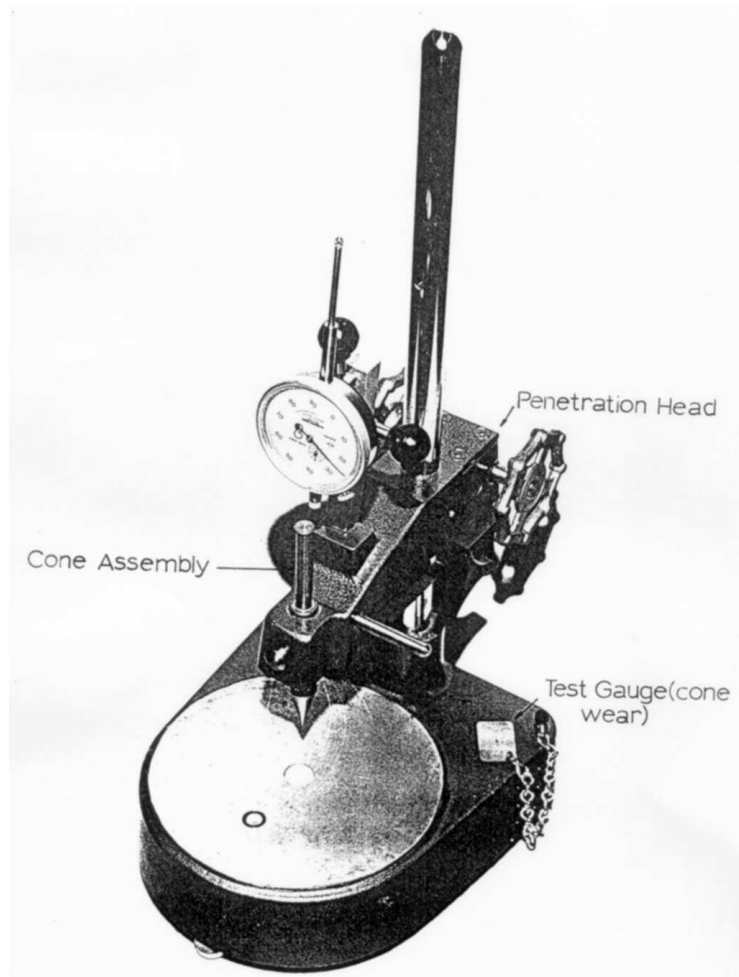


Figure 4-5. Cone penetrometer – apparatus for measuring the cone penetration [9]

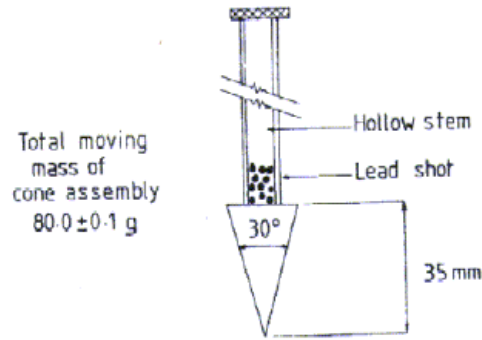


Figure 4-6. Cone standardised geometry and mass [9]

4.2.4. Derived limits

The values of these limits are used in a number of ways. There is also a close relationship between the limits and properties of a soil such as compressibility, permeability, and strength. This is thought to be very useful because as limit determination is relatively simple, it is more difficult to determine these other properties. Thus the Atterberg limits are not only used to identify the soil's classification, but it also allows for the use of empirical correlations for some other engineering properties.

The plasticity index I_P is a measure of the plasticity of a soil. The plasticity index is the size of the range of water contents where the soil exhibits plastic properties. The I_P is the difference between the liquid limit and the plastic limit. Soils with a high I_P tend to be clay, those with a lower I_P tend to be silt, and those with I_P of 0 tend to have little or no silt or clay.

$$I_P = w_L - w_P \quad (1)$$

The liquidity index I_L is used for scaling the natural water content of a soil sample to the limits. It can be calculated as a ratio of difference between natural water content, plastic limit, and plasticity index.

$$I_L = \frac{w - w_P}{I_P} \quad (2)$$

[8]

The consistency index I_c is a ratio of difference between the liquid limit, natural water content, and its plasticity index.

$$I_c = \frac{w_L - w}{I_P} \quad (3)$$

The sum of the consistency and liquidity index must equal to 1.

$$I_L + I_c = 1 \quad (4)$$

4.3. Other Commonly Determinated Soil Properties

4.3.1. Bulk density

The bulk density is a ratio between the mass and the volume of the soil.

$$\rho = \frac{m}{V} \quad (5)$$

4.3.2. Specific weight

The specific weight is a ratio between the mass and the volume of the soil without pores.

$$\rho_s = \frac{m_s}{V_s} \quad (6)$$

This value is obtained by means of *pycnometer* (a small glass flask with a precisely abraded closing, through which is lead a very thin capillary) and distilled water. The density of the water is known, it means that we can simply determine the pycnometer volume (accuracy 0.01 g). The dry soil sample of amount cca 1/4 of the pycnometer volume is perfectly crushed to powder, weighed and placed in the pycnometer, also with water of amount cca half the pycnometer volume. This suspension is boiled for a while in order to get all the air out of the soil (Figure 4-7).



Figure 4-7. Pycnometer with boiling suspension in a sand bath [0]

After, the pycnometer with the suspension is let calm down, filled carefully to the top (the soil fine particles must not flow out!), and closed so that there is no air in the flask. The mass of it can be then determined and compared to the mass of the pycnometer filled just with the distilled water. At this moment, there is enough data to determine the specific weight of the soil.

4.3.3. Wetness

The wetness of a soil is a ratio between mass of water and mass of the dry soil. It is determined by weighing in the wet state, putting in the oven, and weighing in the dry state.

$$w = \frac{m_w - m_d}{m_d} \quad (7)$$

4.4. Maximum Bulk Density

The maximum bulk density is a soil property depending on its moisture content. The soil can be best compacted when it has the maximum bulk density (*optimal moisture content*), which is utilized e. g. in construction of embankments.

The maximum bulk density is determined on the basis of experimental test, when a soil sample is gradually dampened, consistently compacted and weighed. The soil reaches the maximum density, when the sample reaches the highest mass (by sustaining the consistent volume at every soil sample weighing). This procedure is called **The Proctor test**.

Test equipment

- the Proctor mortar and rammer,
- sieve no. 4 (Figure 3-1),
- balance (0,01 kg)
- mixing tools such as mixing pan, spoon, towel, spatula etc,
- moisture device (sprayer),
- straight edge,
- oven.



Figure 4-8. The Proctor mortar and rammer [0]

Procedure

1. Fraction of a dried soil which passes the sieve no. 4 is prepared.
2. The soil is thoroughly mixed with an estimated amount of water (to make it wet cca 6% below the optimal moisture content). A sprayer is used to add the water.
3. This mixture is compacted using the Proctor standard method (compaction in 3 layers giving 25 blows per layer with the 2.5 kg rammer falling through [16]) a few centimetres above the mould–collar interface.
4. The collar is removed, the soil trimmed along the mould top by means of the straight edge, and weighed together with the mould (of which weight is then subtracted).

5. A sample of the soil is taken, weighed, and dried for later determination of the exact wetness (%).
6. The steps above are repeated (the addition of water in step 2 is adequately less and less, as it comes to the wanted moisture content!) until the soil mass starts to diminish or stays constant.

The test results are presented in the bulk density – moisture relationship graph (the regression line obtained from the test values):

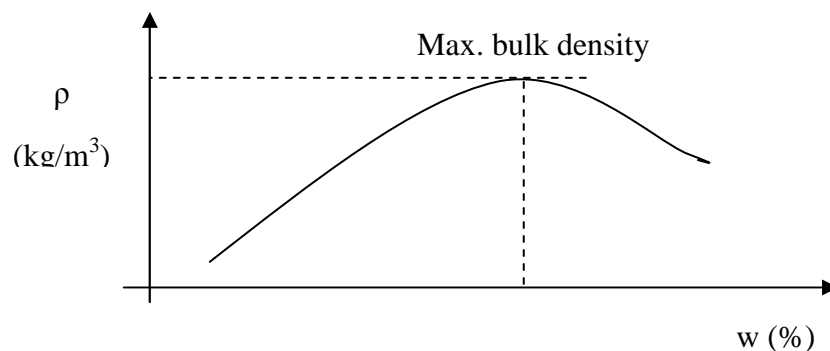


Figure 4-9. Bulk density – moisture relationship, the Proctor test

4.5. Pure Compression (Unconfined Compression)

The unconfined compression determines shear parameters of cohesive soils. In this test, a laterally unsupported cylindrical specimen is subjected to a gradually increased axial compression load until failure occurs. [17]

The unconfined compression strength is defined as the maximum unit axial compressive stress at failure or at 15 percent strain, whichever occurs first.

Test equipment

- Loading Device (triaxial apparatus)
- Measuring equipment, such as dial indicators and callipers
- Timing device

Specimen preparation

Generally, *undisturbed* specimens are prepared from undisturbed tube of a larger size than the test specimen. Specimens must be handled carefully to prevent remoulding, changes in cross section, or loss of moisture. Specimen preparation must be dimensionally accurate. As with triaxial specimens, a membrane is placed over the specimen before loading. If the specimen is not tested

immediately after preparation, precautions must be taken to prevent drying and consequent development of capillary stresses.

The *remoulded* specimen should have the same water content as the undisturbed specimen in order to permit a comparison of the results of the tests on the two specimens. The specimen is compacted in a cylindrical mould with inside dimensions identical with those of the undisturbed specimen. The specimen is carefully removed from the mould and the top of the specimen planed off. The specimen is then ready for testing.



Figure 4-10. Mould for remoulded specimen preparation [0]

Procedure

1. The specimen (covered or uncovered by a rubber membrane) is placed in the loading device so that it is centred on the bottom platen; the loading device is adjusted carefully so that the upper platen barely is in contact with the specimen.
2. The dial indicators are set to zero.
3. The apparatus is started up at desirable axial strain rate (e. g. 1 percent per minute).
4. The progress is recorded (deformation and stress) until the stress starts to decrease (a shear breaking occurs, as proves Figure 4-12) or the deformation reaches 15% of the specimen height (or until desired).

The test results are presented in so-called *stress-strain curve(s)*, which defines the relationship between stress and deformation (proportional deformation).

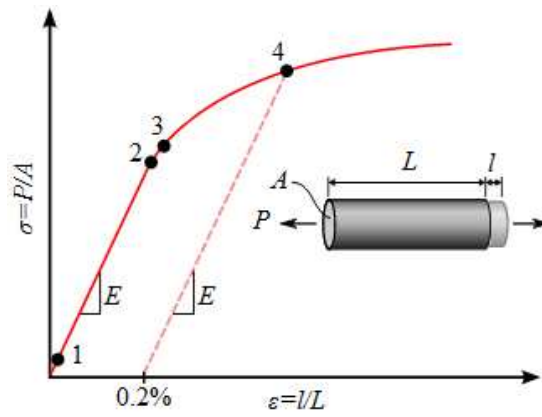


Figure 4-11. Stress-strain curve of a metal (Stress, kPa; strain, %) [18]



Figure 4-12. Shear breaking plane, unconfined compression test of the thesis' sample [0]

4.6. Undrained Triaxial Test

The standard triaxial consolidated undrained test is a confined compression test, in which the soil specimen is first consolidated under all round pressure in the triaxial cell before failure is brought about by increasing the major principal stress.

It may be performed with or without measurement of pore pressure although for most applications the measurement of pore pressure is desirable. [16]

Test equipment

The same as for the unconfined compression plus triaxial cell in which the sample can be subjected to an all round hydrostatic pressure, and hydraulic pressure apparatus including an air compressor and water reservoir in which air under pressure acting on the water raises it to the required pressure, together with the necessary control valves and pressure dials.

Procedure

The same as for the unconfined compression plus these steps between the 1st and 3rd step for the unconfined compression:

1. The specimen is carefully put in the rubber membrane with pressure plates by both sides.
2. The specimen is placed in the compression machine, the both sides sealed by rubber rings.
3. The triaxial cell is laid, properly set up (as described in the unconfined compression test procedure) and uniformly clamped down to prevent leakage of pressure during the test, making sure first that the sample is properly sealed with its end caps and rings (rubber) in position and that the sealing rings for the cell are also correctly placed.
4. When the sample is setup, water is admitted and the cell is fitted under water escapes from the bleed valve, at the top, which is closed.
5. The air pressure in the reservoir is then increased to raise the hydrostatic pressure in the required amount (the vents on the tubes connecting the hydraulic and triaxial cells are open). The pressure gauge must be watched during the test and any necessary adjustments must be made to keep the pressure constant. [16]
6. 2., 3., and 4. step of the unconfined compression test procedure.



Figure 4-13. Specimen prepared for triaxial test [0]

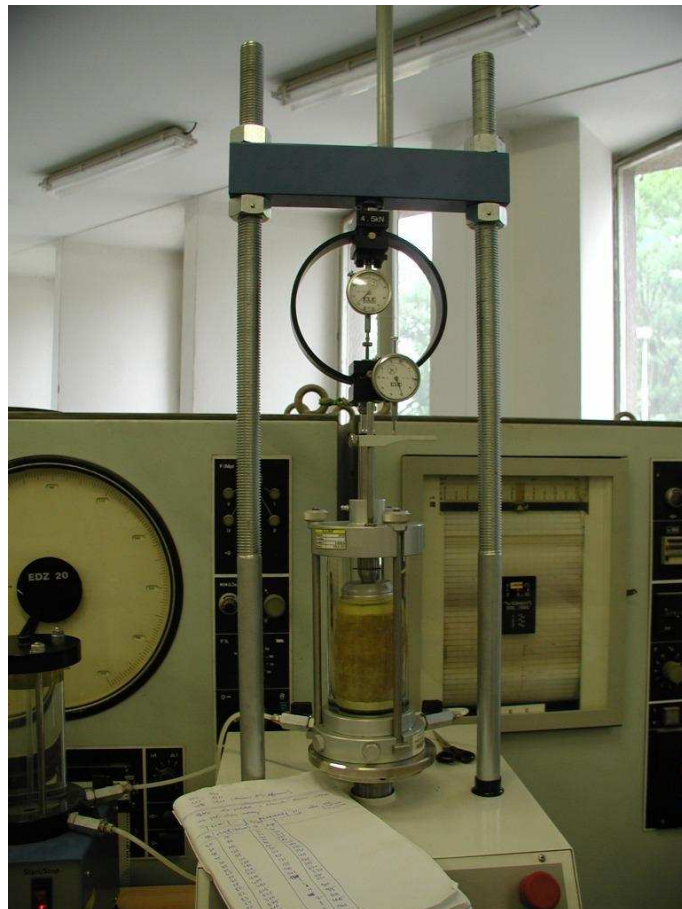


Figure 4-14. Triaxial running the thesis' soil specimen [0]

The test results are similar to the previously described, with the difference of the side pressure.

The strain and corresponding stress is plotted with stress abscissa and curve is drawn. The maximum compressive stress at failure and the corresponding strain and cell pressure are found out.

The stress results of the series of triaxial tests at increasing cell pressure are plotted on a mohr stress diagram. In this diagram a semicircle is plotted with normal stress and abscissa shear stress as ordinate.

The condition of the failure of the sample is generally approximated by a straight line drawn as a tangent to the circles, the equation of which is

$$\tau = C + \sigma \tan \varphi \quad (8)$$

where τ is shear stress, σ is normal (σ_{max} or σ_1 is axial, σ_{min} or σ_3 is side, chamber) stress, value of cohesion C is read of the shear stress axis, where it is cut by the tangent to the mohr circles, and the *angle of shearing resistance* φ (*peak friction angle*) is angle between the tangent and a line parallel to the normal (axial) stress. [16]

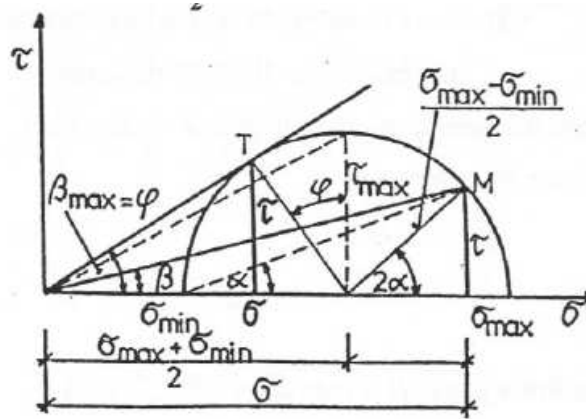


Figure 4-15. The Mohr circle [19]

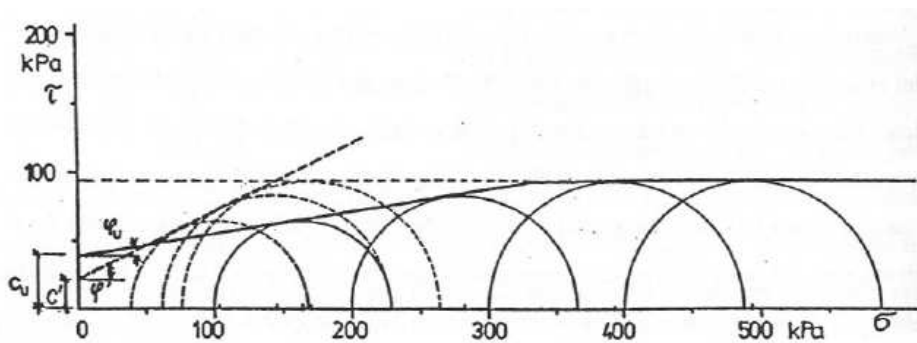


Figure 4-16. Evaluation of the triaxial test [19]

PART TWO: Laboratory Research

soil & fibre material, characterisations and tests

5. Laboratory Instrumentation

This chapter lists and briefly describes the faculty laboratory instrumentation which was utilized in the thesis' laboratory research.

Triaxial ELE Multiplex 50, 25-3700

Specification

Dimensions (l x w x h) 550 mm x 400 mm x 1230 mm

Max. vertical clearance (platen down crosshead up) 795 mm

Min. vertical clearance (platen up crosshead down) 210 mm

Horizontal clearance 265 mm

Platen diameter 133.3 mm

Platen adaptor diameter 158.5

Platen travel 100 mm (nominal)

Platen speed Variable 0.5 to 50.8 mm/min
(0.020 – 2 in/min)

Weight 71 kg

Load ring capacity 25 kN



Figure 5-1. Triaxial ELE Multiplex 50 [0]

[20]

Balance Kern 600-2M

Accuracy: 0.01 g.

Capacity: 600 g.

[21]



Figure 5-2. Kern 600-2M [21]



Figure 5-3. Balance Kern DE60K20 [0]

Balance Kern DE60K20

- PLATFORM BALANCE, 60.0KG
- Resolution, weight:20g
- Weight, load max:60kg
- Accuracy, + percentage:20%
- IP rating:54
- Length / Height, external:310mm
- Range:60kg
- Weight, calibration:60kg

[22]

Oven Venticell 111

- 111-liter chamber volume.
- Working temperature of from +10°C over ambient temperature up to 250°C. [23]



Figure 5-4. Oven Venticell 111 [0]

6. Specimen Laboratory Testings

This chapter is devoted to the core of the bachelor thesis itself: exploring properties of soil, reinforced soil by the fibres, and their mutual comparison and evaluation. On the basis of it, the fibre-reinforcement technique can be identified and evaluated.

The chapter comprises data acquired from the tests, tests results and evaluations. Tests equipments, preparation, procedures, and computations are described in chapter 4, Laboratory Tests.

6.1. Soil Specimen Elementary Characterisation

SPECIMEN DENSITY AND WETNESS

m_s (g)	m_d	Dimensions of the sample (cylinder)	d (mm)	81.6	ρ (kg/m ³)	2063.174
394.9	323.96		h (mm)	36.6	w (%)	21.89777
			V (mm ³)	191404.1211		

Figure 6-1. Determination of specimen density and wetness

(Where m_s is specimen mass in natural state, m_d dry specimen mass, w wetness in natural state.)

The specimen wetness was determined according to the relationship (7) **21.90%** and the density (5) **2063.17 kg/m³**.

LIQUID LIMIT

Specimen	m_b (g)	$m_b + m_s$	m_s	penetration (mm)	$m_d + m_b$	m_d	w (%)
1	116.90	156.47	39.57	17.00	140.86	23.96	65.15
2	117.51	172.06	54.55	16.70	150.36	32.85	66.06
3	77.93	132.91	54.98	17.70	111.15	33.22	65.50
4	76.80	125.61	48.81	20.50	105.76	28.96	68.54
5	123.06	158.65	35.59	20.20	144.29	21.23	67.64
6	115.92	159.60	43.68	19.10	142.20	26.28	66.21

Figure 6-2. Data for determining liquidity limit

(Where b means bowl.)

The liquid limit is achieved when the penetration cone penetrates to 20 mm depth to the soil. To get the „exact“ result, the data are plotted in a graph and a regressive curve is constructed.

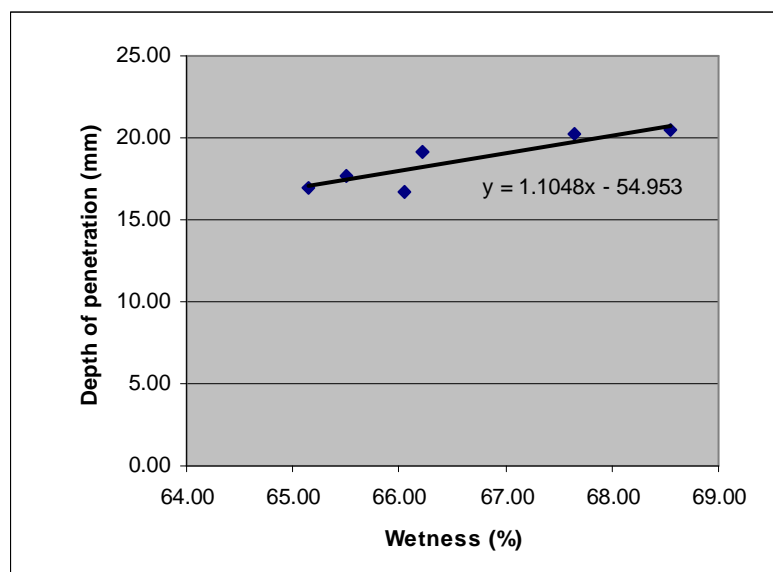


Figure 6-3. Regressive curve for obtaining the liquidity limit

According to the regression curve, the wetness (a value on the x axis) is 67.8 for the depth of penetration (on the y axis) of 20.

The liquid limit is **67.8%**.

PLASTIC LIMIT

m_b (g)	$m_{pl} + m_b$	m_{pl}	$m_{pl,d} + m_b$	m_d	w_p (%)
117.3	118.51	1.21	118.23	0.93	30.11

Figure 6-4. Plastic limit data

The plastic limit is **30.11%**.

INDEXES

Plasticity index was computed according to the equation (1) $I_p = 37.74$, liquidity index (2) $I_L = -0.22$, and consistency index (3) $I_C = 1.22$.

6.2. Standard Proctor Test

mortar kg	mortar + soil kg	soil kg	bowl g	bowl + soil g	soil g	bowl + dry soil g	dry soil g	wetness %	density (ρ) kg/m ³
4.30	6.00	1.70	111.70	320.60	208.90	284.94	173.24	20.58	1812.12
4.30	6.06	1.76	110.68	246.25	135.57	218.40	107.72	25.85	1876.08
4.30	6.10	1.80	111.95	222.04	110.09	197.02	85.07	29.41	1918.72
4.30	6.04	1.74	107.05	327.69	220.64	273.31	166.26	32.71	1854.76

Figure 6-5. Standard Proctor test data

The wetness is computed according to (7).

Likewise in the liquid limit test, there was a need to construct the regressive curve in order to read the maximum density value.

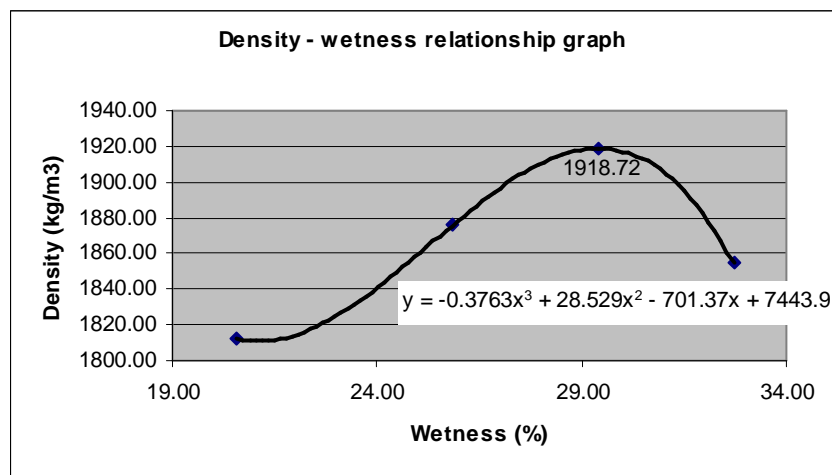


Figure 6-6. Regressive curve for determining the optimal wetness

The regressive curve indicates that the x for y maximum equals **29.41%** (the highest y value is identical to the value in the table above).

6.3. Pycnometer Test (Specific Weight)

m_{pyc}	$m_{pyc+water}$	m_{water}	$m_{pyc+dry\ soil}$	$m_{dry\ soil}$	boiled → $m_{pyc+soil+water}$	$m_{soil+water}$	$m_{soil+water-soil}$
53.89	151.12	97.23	82.13	28.24	168.68	114.79	86.55

Figure 6-7. Specific weight, measured data

Input data

ρ_{water} (g/cm ³)	1
V_{pyc} (cm ³)	97.23
V_{soil} (cm ³)	10.68

Relationships (based on (5) and (6))

$$V_{pyc} = \frac{m_{water}}{\rho_{water}}$$

$$V_{soil} = \frac{m_{water} - m_{soil+water-soil}}{\rho_{water}}$$

$$m_{\text{specif}} (\text{g/cm}^3) = \boxed{2.64} \qquad m_{\text{specif}} = \frac{m_{\text{soil}}}{V_{\text{soil}}}$$

The specific weight of the specimen is **2.64 g/cm³**.

6.4. Grain Size Analysis

The soil sample was of very fine clayey fractions, therefore the sedimentation technique of the grain size analysis was employed. The following equations describes the unique empirical relationships among the velocity of particles, which vary in sizes, sedimentation, hydrometer gauge reading and calibration, temperature of the suspension and its density, etc.

Hydrometer

$$h_{op} = R'_h + t_m \qquad \text{where } h_{op} \dots \text{hydrometer gauge reading translation (h corrected)}^*,$$

$$R'_h \dots \text{hydrometer gauge reading,}$$

$$t_m \dots \text{temperature correction (Figure 6-8).}$$

8	-0,0013	20	+0,0000
9	-0,0013	21	+0,0002
10	-0,0013	22	+0,0004
11	-0,0012	23	+0,0006
12	-0,0012	24	+0,0008
13	-0,0011	25	+0,0010
14	-0,0009	26	+0,0013
15	-0,0008	27	+0,0015
16	-0,0006	28	+0,0018
17	-0,0005	29	+0,0020
18	-0,0003	30	+0,0023
19	-0,0002	31	+0,0026

Figure 6-8. Temperature correction chart [7]

Hydrometer calibration relationship

$$h_r = 186,24 - 3,9179 \cdot h_{op} \qquad \text{where } h_r \dots \text{“effective depth“.}$$

Equivalent particle diameter d_i

$$d_i = 0,005531 \cdot \sqrt{\frac{\eta \cdot h_r}{(\rho_s - 1) \cdot t}} \qquad \text{where } \eta \dots \text{dynamic viscosity, viz. Figure 6-9}$$

* (hop - 1000)*1000 is employed in calculation further.

Dynamic viscosity values	
t (°C)	η (mPa*s)
10	1.304
15	1.137
20	1.002
25	0.891
30	0.798

Figure 6-9. Dynamic viscosity according to temperature [7]

The values between can be achieved by constructing and expressing a regressive curve:

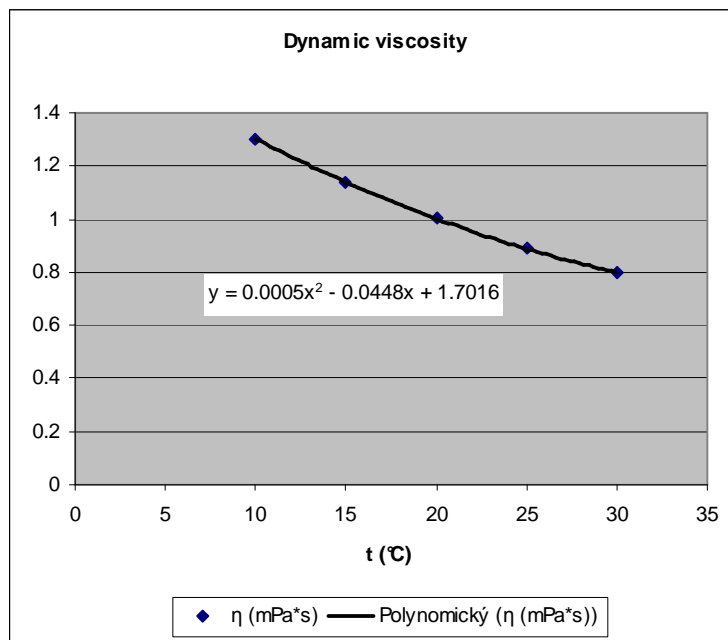


Figure 6-10. Dynamic viscosity – temperature relationship according to the table above

Weight portion of fraction diameters less than d_i

$$K = \frac{100 \cdot \rho_s \cdot h_{op}}{m \cdot (\rho_s - 1)} \quad [7]$$

Mass and diameter of the soil powder added to the 1000 ml graduated cylinder

g	g	g	mm	g/cm ³
bowl + soil	bowl	soil	sieve	specific weight ρ_s
194.64	165	29.64	0.06	2.64

Figure 6-11. Sedimentation technique, input data

Test progress data

time (min)	time (s)	R'h	t (°C)	hop	hr	η	d_i (mm)	K (%)	(h_{op} supplied)
	5	1.0178	21.93	1.0182	182.2508	0.9596	0.0255	98.6732	18.1860
	10	1.0176	21.93	1.0180	182.2516	0.9596	0.0180	97.5880	17.9860
	30	1.0174	21.94	1.0178	182.2524	0.9594	0.0104	96.5137	17.7880
	60	1.0172	21.95	1.0176	182.2532	0.9591	0.0074	95.4394	17.5900
2	120	1.0163	21.96	1.0167	182.2567	0.9589	0.0052	90.5671	16.6920
4	240	1.0158	22.00	1.0162	182.2586	0.9580	0.0037	87.8976	16.2000
8	480	1.0098	22.06	1.0102	182.2821	0.9566	0.0026	55.4080	10.2120
10	600	1.0068	22.09	1.0072	182.2938	0.9560	0.0023	39.1633	7.2180
14	840	1.0012	22.15	1.0016	182.3157	0.9546	0.0020	8.8440	1.6300
20	1200	0.9991	22.25	0.9996	182.3239	0.9523	0.0016	-	
30	1800	0.9986	22.40	0.9991	182.3257	0.9490	0.0013	-	
60	3600	0.9984	22.84	0.9990	182.3261	0.9392	0.0009	-	
120	7200	0.9980	23.60	0.9987	182.3271	0.9228	0.0007	-	
240	14400	0.9980	24.25	0.9989	182.3266	0.9092	0.0005	-	

Figure 6-12. Hydrometer test, data measured and computed

Weight portion of diameter less than and equal d_i max (it means the total) should be mathematically 100%. The more the value is nearer, the more the test was successful. In this case the total is 98.67%.

A common and transparent information describing the grain size distribution gives a grain size curve (ČSN CEN ISO/ITS 17892-4):

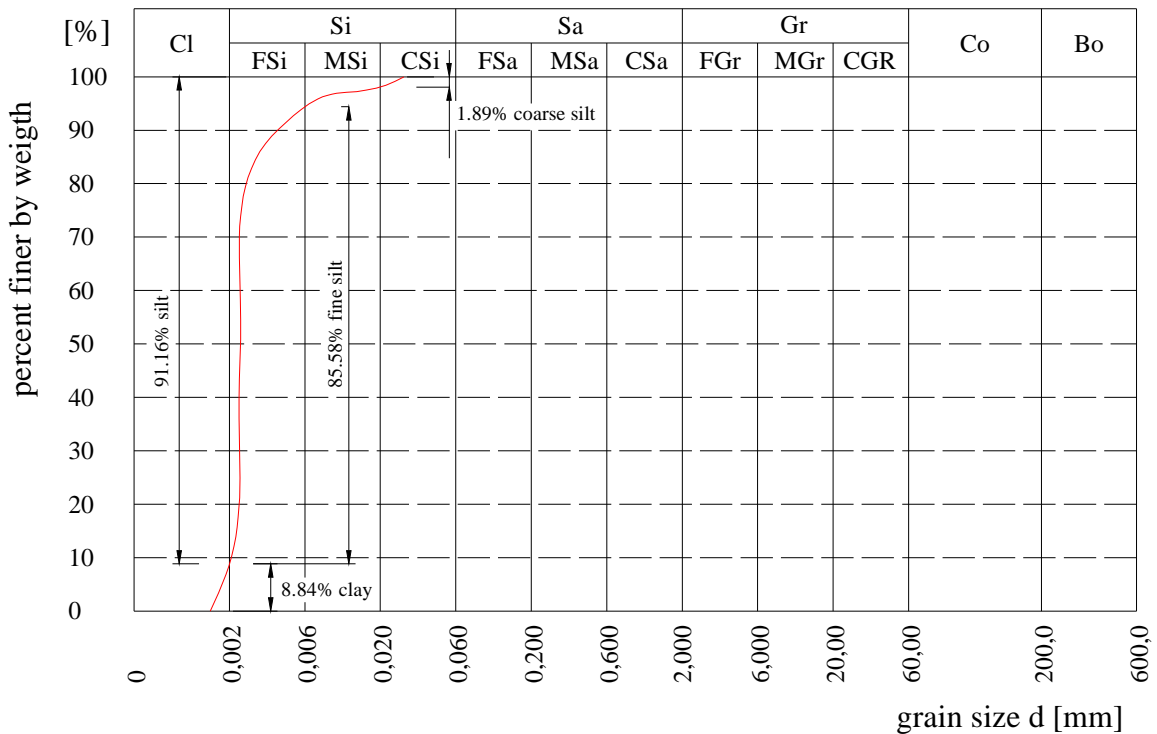


Figure 6-13. Grain size curve of the thesis' soil sample

6.5. Specimen Classification

Enough tests for the specimen classifying were performed. It is now possible to determine, to which kind of soil the specimen belongs. The soil classification is discussed in chapter 3 in detail.

Thus the **specimen employed in this thesis belongs** according to the plasticity chart (Figure 3-4), according to the triangular diagram (used in the Czech Republic, Figure 3-5) to **the group SH: „Elastic inorganic silt with moderate to high plasticity“** (USCS, Figure 3-2), or to the group **clSi** (Figure 3-5).

6.6. Pure Compression

Specimen characterisation

The specimen is cylinder-shaped. Moisture was added – the aim was to moisten the specimen to get the optimal moisture content (29.41%) assessed by the Proctor test, chapter 4.4.

d (diameter, mm)	40
h (height, mm)	80
w (wetness, %)	30.2

Determination of normal stress

The values were computed according to the elementary physical relationship:

$$\sigma = \frac{F}{A} \quad \text{where } F \dots \text{force affecting the specimen,} \quad (9)$$

$A \dots$ area subjected to the force,

which is in case of a cylinder defined

$$A = \pi r^2 \quad (10)$$

Taken from these relationships and the calibration curve for the measuring ring (Figure 6-15), the definite equation for determining the main (normal, vertical) stress has this image:

$$\sigma = \frac{0.003 \cdot GR + 0.0237}{\pi \frac{d^2}{4}} \cdot 10^6 \quad (kPa) \quad (11)$$

where $GR \dots$ Gauge Reading from the triaxial load ring.

Load (kN)	Gauge reading
0.0	0.0
0.6	191.4
0.8	257.7
1.2	387.8
1.6	519.4
2.0	652.1
2.4	783.0
2.8	918.1
3.2	1050.5
3.6	1186.4
4.0	1320.6
4.5	1489.0

Figure 6-14. Calibration chart for the measuring ring

The calibration chart was transferred into the calibration function in order to get all the values needed.

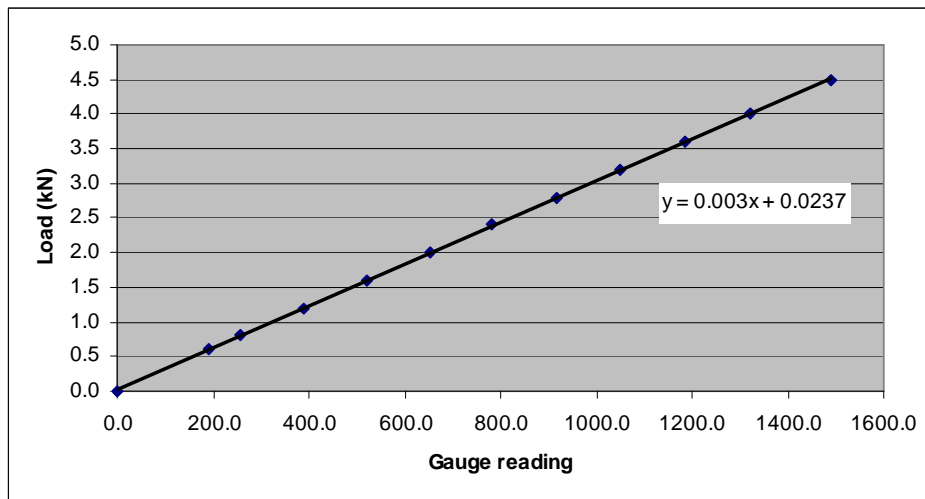


Figure 6-15. Calibration curve for the measuring ring

Test progress data

Annotation	Units
G. R...Gauge Reading	-
Def...Deformation	0.1 mm
Stress...normal (axial) stress	kPa
Specimen no.– in coloured cells	
Speed of deformation	1 mm/min

1			2			3		
Def.	G. R.	≈ Stress	Def.	G. R.	≈ Stress	Def.	G. R.	≈ Stress
4	10	42.73	2	8	37.96	4	8	37.96
5	11	45.12	4	10	42.73	6	10	42.73
8	13	49.90	6	11	45.12	8	11	45.12
9	14	52.28	8	13	49.90	10	12	47.51

1			2			3		
Def.	G. R.	≈ Stress	Def.	G. R.	≈ Stress	Def.	G. R.	≈ Stress
10	15	54.67	10	14	52.28	14	14	52.28
11	16	57.06	12	15	54.67	16	15	54.67
13	17	59.44	14	16	57.06	19	16	57.06
15	19	64.22	16	17	59.44	21	17	59.44
17	20	66.61	17	18	61.83	23	18	61.83
18	21	68.99	20	19	64.22	26	19	64.22
20	22	71.38	22	20	66.61	28	20	66.61
22	23	73.77	25	21	68.99	31	21	68.99
24	24	76.16	28	22	71.38	34	22	71.38
25	25	78.54	30	23	73.77	38	23	73.77
28	26	80.93	33	24	76.16	41	24	76.16
29	27	83.32	36	25	78.54	44	25	78.54
33	29	88.09	40	26	80.93	48	26	80.93
35	30	90.48	42	27	83.32	52	27	83.32
38	31	92.87	45	28	85.70	57	28	85.70
41	32	95.25	49	29	88.09	62	29	88.09
44	33	97.64	52	30	90.48	69	30	90.48
47	34	100.03	56	31	92.87	90	31	92.87
50	35	102.42	59	32	95.25	100	30	90.48
53	36	104.80	64	33	97.64			
56	37	107.19	68	34	100.03			
60	38	109.58	72	35	102.42			
65	39	111.97	78	36	104.80			
73	40	114.35	83	37	107.19			
90	41	116.74	92	38	109.58			
100	39	111.97	100	39	111.97			
			115	39	111.97			
			120	38	109.58			

Figure 6-16. Pure compression test, data measured and computed

The specimens average stress bearing capacity is given by the arithmetic mean of the highest Stress values, which is **107 kPa**.

Acquired data were plotted in the stress-deformation graph for single specimens:

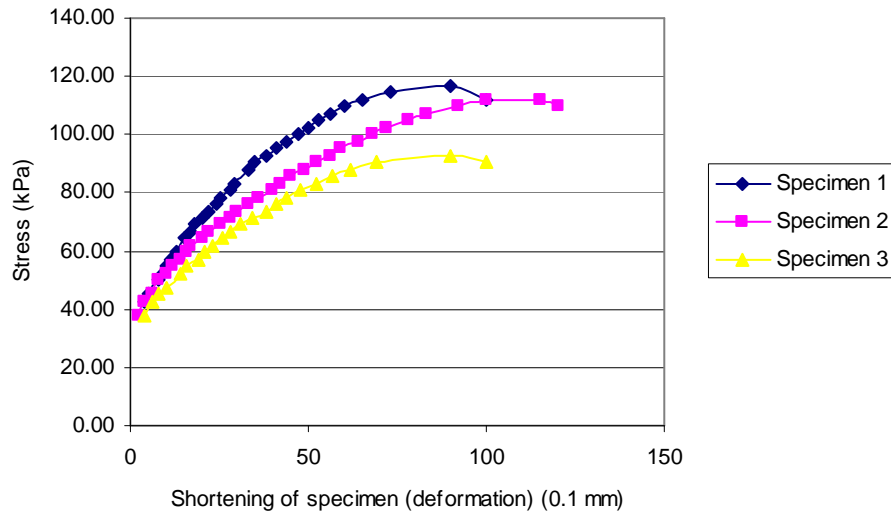


Figure 6-17. Pure compression test, stress-deformation curves

As obvious from the graph, the duration of the specimen behaviour under graduating stress is a smooth, nonlinear, gradually less growing function, until the point of the bearing capacity, where the function growth stops and usually starts to fall rapidly.

6.7. Triaxial Compression

6.7.1. Unreinforced Soil Testing

Specimen characterisation

d (diameter, mm)	60
h (height, mm)	120
w (wetness, %)	26.2

Side pressure – pressure in the triaxial chamber

Specimen	1	2	3	4
$\bar{\sigma}_3$ (side pressure, kPa)	0 (pure compression)	150	150	400

Test progress data

Annotation	Units
G. R...Gauge Reading	-
Def...Deformation	0.1 mm
$\bar{\sigma}_1 - \bar{\sigma}_3$...Stress deflector	kPa
Specimen no. - in coloured cells	
Speed of deformation	1 mm/min

1			2			3			4		
Def.	G. R.	$\bar{\sigma}_1 - \bar{\sigma}_3$	Def.	G. R.	$\bar{\sigma}_1 - \bar{\sigma}_3$	Def.	G. R.	$\bar{\sigma}_1 - \bar{\sigma}_3$	Def.	G. R.	$\bar{\sigma}_1 - \bar{\sigma}_3$
2	10	18.99	2	20	29.60	10	20	29.60	3.5	30	40.21
5.5	20	29.60	4.3	40	50.82	13	40	50.82	6	50	61.43
7.5	30	40.21	9	60	72.04	18	60	72.04	11	70	82.65
12	40	50.82	15	80	93.26	25	80	93.26	14.5	80	93.26
15	45	56.13	23	100	114.49	37	100	114.49	24	100	114.49
17	50	61.43	25.5	105	119.79	51	115	130.40	30	110	125.10
19	55	66.74	31	115	130.40	60	120	135.71	38.5	120	135.71
22	60	72.04	34	120	135.71	75	130	146.32	49	130	146.32
25	65	77.35	38	125	141.01	91	135	151.62	61.5	140	156.93
28.5	70	82.65	42.5	130	146.32	111	138	154.80	81	150	167.54
32	75	87.96	48	135	151.62	139	137	153.74	101	155	172.84
34.5	78	91.14	53	139	155.87	150	136	152.68	106	156	173.90
36	80	93.26	54.5	140	156.93				115	157	174.96
38	82	95.39	59	143	160.11				130	158	176.03
40	85	98.57	63	145	162.23				145	157	174.96
44	88	101.75	72	148	165.42				152	156	173.90
46	90	103.88	76.5	149	166.48						
48	92	106.00	80	150	167.54						
52	95	109.18	84	151	168.60						
59.5	100	114.49	90	152	169.66						
64	102	116.61	95.5	153	170.72						
70	105	119.79	105	154	171.78						
77	107	121.91	112	155	172.84						
84	109	124.03									
100	108	122.97									
101.5	107	121.91									
103.5	105	119.79									

Figure 6-18. Triaxial test of unreinforced soil, data measured and computed

Where $\bar{\sigma}_1 - \bar{\sigma}_3$ is a difference between the principal stresses – axial (normal) and side (chamber – induced by water in the triaxial chamber).

The test with 150 kPa side pressure was conducted 2 times, thus the values are represented by an average stress value, which is 163.82 kPa.

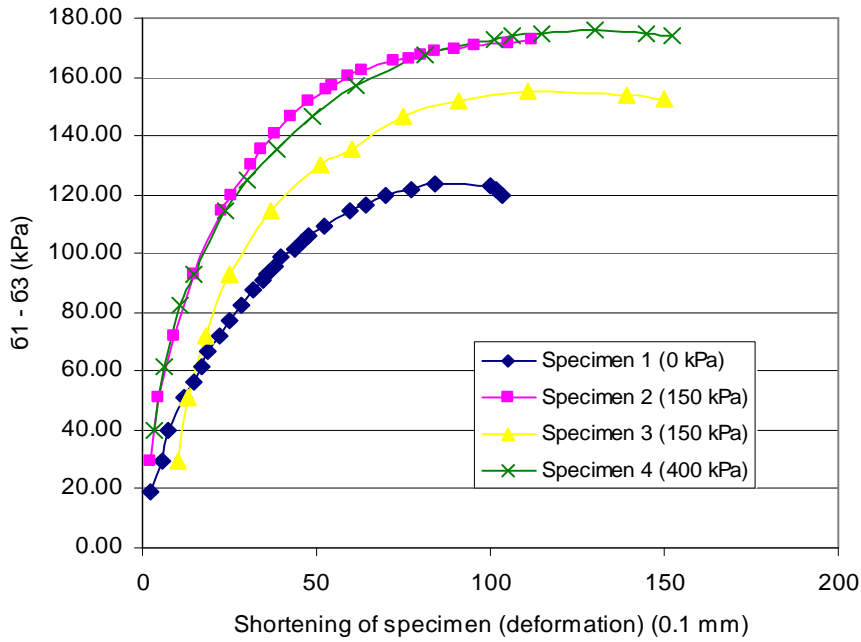


Figure 6-19. Triaxial test of unreinforced soil, stress-deformation curves

Specimens 1, 2 and 3 exhibit growth of the bearing capacity, when affected by growing of the side pressure.

6.7.2. Reinforced Soil Testing

This chapter shows behaviour of fibre-reinforced soil samples (by means of triaxial tests, again) and compares the results with some research tests, which have been conducted.

First, the reinforcing polypropylene fibres utilized in these tests, as well as a methodology of the specimen reinforcing and preparation should be discussed.

POLYPROPYLENE FIBRILLATED FIBRES TEXSOL

As already mentioned, this product is made by Kordárna, a. s., Velká nad Veličkou, Czech Republic. [24] Its strength and deformation properties shows Figure 6-21.

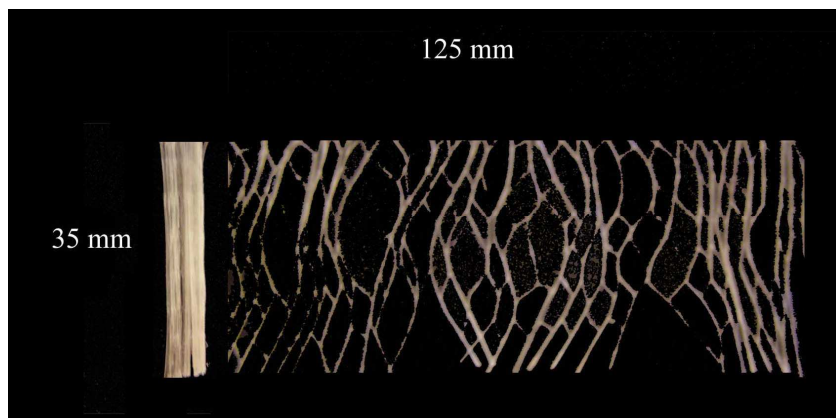


Figure 6-20. Widht extension of the fibres [24]

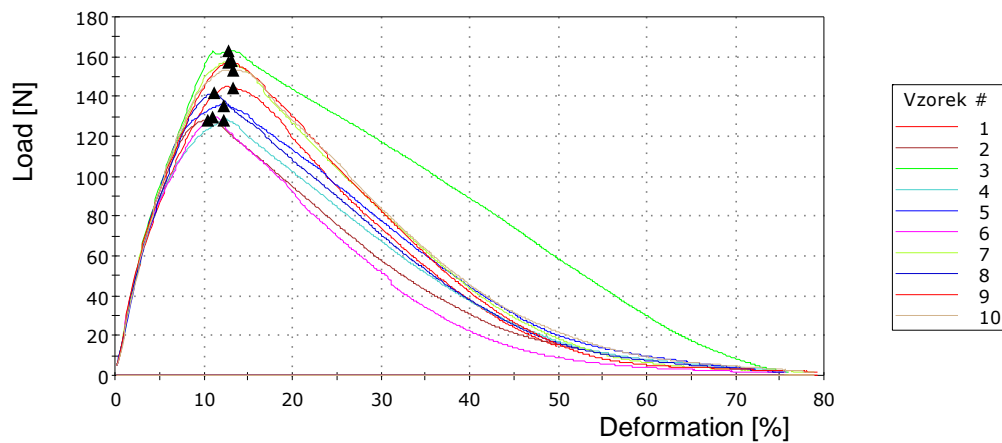


Figure 6-21. Mechanical property of the Texsol fibres [24]

Methodology

Using fibres random distribution technique, soil is usually reinforced by the fibre mass amount of tenths of percent of the soil mass amount. The fibres volume content for reinforcement of the tested specimens was set at 0.5% and 1% of fibres mass of the moistened soil mass. Again, the soil is moistened at the optimal moisture content – the maximum bulk density.

Specimen preparation

The fibres were mixed into a dry soil. The required moisture was gradually added, while keeping mixing. In order to disperse the fibres thoroughly, the mixing was made by hands; at the beginning, when the soil is dry or semidry, the fibres are rubbed together with the soil between palms so that they are extended along their width. After the fibres were dispersed well, the mixture was let consolidate for a while. Next, the cylinder-shaped specimen is prepared as described in chapter 4.5.

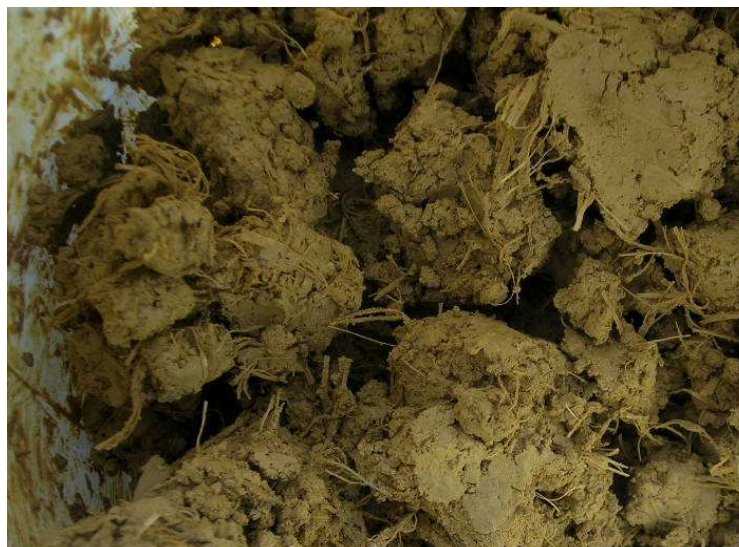


Figure 6-22. Mixture of soil and fibres [0]

6.7.2.1. Test I. 0.5% Reinforcement

Specimen characterisation

d (diameter, mm)	60
h (height, mm)	120
w (wetness, %)	29.9
Reinforcement (%)	0.5

Test progress data

Specimen	1	2	3	4
σ_3 (side pressure, kPa)	0 (pure compression)	0	150	400
Speed of deformation	1 mm/min			

1	2	3			Stress deflector $\sigma_1 - \sigma_3$ (kPa)	4			Stress deflector $\sigma_1 - \sigma_3$ (kPa)
0	0	150	Gauge Reading	\approx Load (kN)		400	Gauge Reading	\approx Load (kN)	
Deformation (0,1 mm)						Deform.			
3		3	20	0.08	29.60	12	40	0.14	50.82
6	4	8	30	0.11	40.21	13.5	50	0.17	61.43
		12.5	35	0.13	45.52	16	60	0.20	72.04
10.5			37	0.13	47.64	17	75	0.25	87.96
13			40	0.14	50.82	19	85	0.28	98.57
15		16.5	42	0.15	52.95	20	90	0.29	103.88
16.5			44	0.16	55.07	22.5	100	0.32	114.49
		21	45	0.16	56.13	25.5	110	0.35	125.10
18.5			46	0.16	57.19	28.5	120	0.38	135.71
		24	48	0.17	59.31	32	130	0.41	146.32
22.5	22	27	50	0.17	61.43	39	145	0.46	162.23
25			52	0.18	63.56	41.5	150	0.47	167.54
		31	53	0.18	64.62	49	160	0.50	178.15
			54	0.19	65.68	57	170	0.53	188.76
28		34	55	0.19	66.74	63	175	0.55	194.06
			56	0.19	67.80	70	180	0.56	199.37
		37	57	0.19	68.86	79	185	0.58	204.67
32.5			58	0.20	69.92	90	190	0.59	209.98
		41	59	0.20	70.98	94	191	0.60	211.04
36	39	43	60	0.20	72.04	99	192	0.60	212.10
39.5		46	62	0.21	74.17	110	195	0.61	215.28
42			63	0.21	75.23	114	196	0.61	216.34
44			64	0.22	76.29	121	197	0.61	217.41
46.5	60	55	65	0.22	77.35	128	198	0.62	218.47
	73		65	0.22	77.35	136	199	0.62	219.53
50.5		60	66	0.22	78.41	147	200	0.62	220.59
65		66	67	0.22	79.47	155	201	0.63	221.65
		70	68	0.23	80.53	162	202	0.63	222.71
		80	69	0.23	81.59	173	203	0.63	223.77
		86	68	0.23	80.53	190	205	0.64	225.89
		92	67	0.22	79.47	Achieved 15% of axial deformation (18 mm), test ended.			

1	2	3			Stress deflector $\sigma_1 - \sigma_3$ (kPa)	4			Stress deflector $\sigma_1 - \sigma_3$ (kPa)
0	0	150	Gauge Reading	\approx Load (kN)		400	Gauge Reading	\approx Load (kN)	
Deformation (0,1 mm)						Deform.			
		100	66	0.22	78.41				
			65	0.22	77.35				
	78	106	64	0.22	76.29				
		137	64	0.22	76.29				
		147	65	0.22	77.35				
73	82		63	0.21	75.23				
76	88		62	0.21	74.17				
	95		61	0.21	73.11				
	102		61	0.21	73.11				
86	119		60	0.20	72.04				
90	134		59	0.20	70.98				
	140		58	0.20	69.92				
95.5	144		57	0.19	68.86				
99.5	149		56	0.19	67.80				
104	154		55	0.19	66.74				
108			53	0.18	64.62				
113.5			50	0.17	61.43				
			75	0.25	87.96				
			85	0.28	98.57				
			90	0.29	103.88				
			100	0.32	114.49				

Figure 6-23. Triaxial test of 0.5% reinforced soil I, data measured and computed

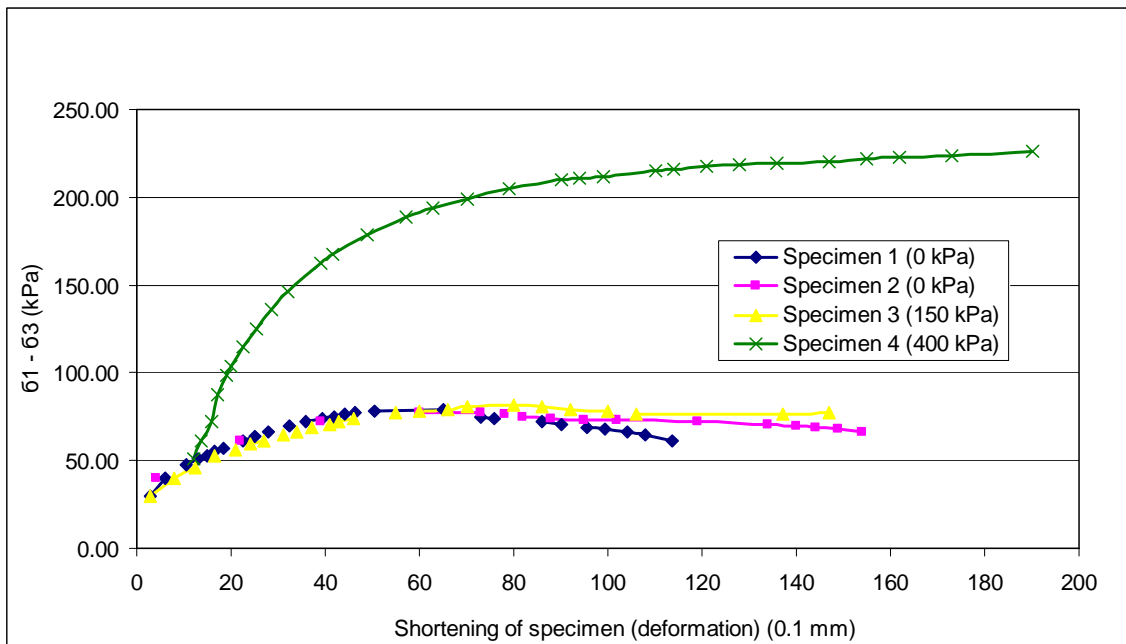


Figure 6-24. Triaxial test of 0.5% reinforced soil, stress-deformation curves



Figure 6-25. Reinforced specimens after triaxial test (1) unconfined (2) confined compression [0]



Figure 6-26. Shear breaking plane, reinforced specimen [0]

The result doesn't indicate any improvement, when compared with (Figure 6-19. Triaxial test of unreinforced soil, stress-deformation curves). The green curve even didn't reach a peak strength state, which can explain a wrong specimen position in triaxial or other imperfections.

However, certain difference is in the smoother curves durations, which is caused by the reinforcement. Test II. 0.5% Reinforcement

Specimen characterisation

Specimen characterisation	
d (diameter, mm)	60
h (height, mm)	120
w (wetness, %)	34.5
Reinforcement (%)	0.5
Speed of deformation	1 mm/min

Specimen	1	2
$\bar{\sigma}_3$ (side pressure, kPa)	150	400

Test progress data

0.1 mm	1	kPa	0.1 mm	2	kPa
Deform.	G. R.	$\bar{\sigma}_1 - \bar{\sigma}_3$	Deform.	G. R.	$\bar{\sigma}_1 - \bar{\sigma}_3$
4.5	35	45.52	4	40	50.82
8	50	61.43	7.3	60	72.04
11	60	72.04	12.5	80	93.26
15	70	82.65	15.5	90	103.88
19.5	80	93.26	20	100	114.49
25	90	103.88	25.5	110	125.10
32.5	100	114.49	28.5	115	130.40
36.5	105	119.79	32	120	135.71
43	110	125.10	37.5	125	141.01
50	115	130.40	43.5	130	146.32
62	120	135.71	52	135	151.62
73	121	135.77	54.5	136	152.68
78	120	135.71	56.5	137	153.74
85	119	134.65	59	138	154.80
92	118	133.58	67.5	140	156.93
			73.5	141	157.99
			78.5	142	159.05
			96	143	160.11
			110	144	161.17
			118	143	160.11
			135	142	159.05

Figure 6-27. Triaxial test of 0.5% reinforced soil II, data measured and computed

The graph shows Test II results (Specimens 1 and 2) in comparison with Triaxial test of unreinforced soil, Figure 6-19.

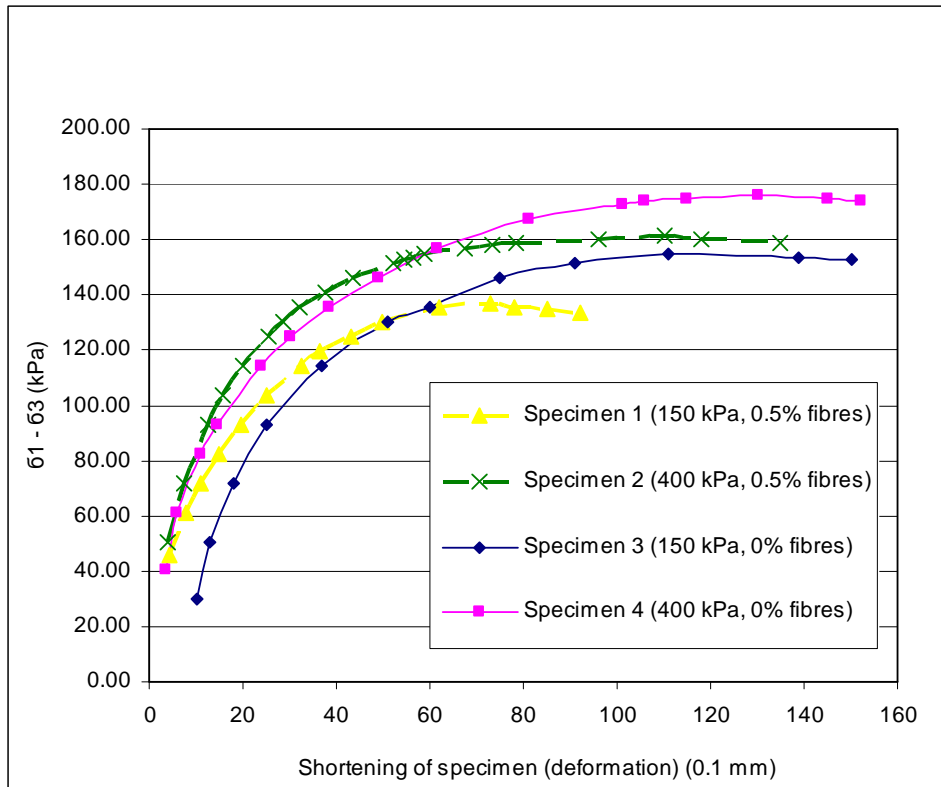


Figure 6-28. Stress-deformation curves of reinforced and unreinforced triaxial-tested samples

The graph results show that both the reinforced and unreinforced soils intersect at the point of axial deformation of approximately 6 mm (5%). The stress-strength reaction of the reinforced specimens is higher that of unreinforced ones until this point. The reinforced specimens' strength then slowly starts to decrease, while the unreinforced specimens' continue increasing.

The bearing capacity of the reinforced specimens is lower than of the unreinforced ones.

Specimen 1 and 2 have 34.5% wetness (!), specimens 3 and 4 only 26.2% (!). The optimal wetness should be 29.4%.

The specimens are subjected to the confined stress.

6.7.2.2. Test III. 1% Reinforcement

Specimen characterisation

d (diameter, mm)	60
h (height, mm)	120
w (wetness, %)	31.6
Reinforcement (%)	1.0

Test progress data

Deformation speed (mm/min)	1
----------------------------	---

Specimen	1	2	3
$\bar{\sigma}_3$ (side pressure, kPa)	0	150	400

1	2				3			
Jaw shift (0,1 mm)	Gauge Reading	\approx Load (kN)	$\bar{\sigma}_1 - \bar{\sigma}_3$ (kPa)	Jaw shift	Gauge Reading	\approx Load (kN)	$\bar{\sigma}_1 - \bar{\sigma}_3$	
3.5		20	0.08	29.60	11	90	0.29	103.88
7	4	30	0.11	40.21	14	100	0.32	114.49
11		40	0.14	50.82	17	110	0.35	125.10
13.5		45	0.16	56.13	22.5	125	0.40	141.01
16.5	7.5	50	0.17	61.43	25	130	0.41	146.32
20		55	0.19	66.74	29.5	140	0.44	156.93
23.5		60	0.20	72.04	36.5	150	0.47	167.54
28		65	0.22	77.35	45	160	0.50	178.15
32	12.5	70	0.23	82.65	50	165	0.52	183.45
37.5		75	0.25	87.96	56	170	0.53	188.76
41.5		78	0.26	91.14	64.5	175	0.55	194.06
45	15	80	0.26	93.26	74	180	0.56	199.37
49		82	0.27	95.39	79	182	0.57	201.49
51.5		83	0.27	96.45	81	183	0.57	202.55
53.5		84	0.28	97.51	88	184	0.58	203.61
55		85	0.28	98.57	94	185	0.58	204.67
57.5		86	0.28	99.63	97	186	0.58	205.73
61		87	0.28	100.69	104	187	0.58	206.80
64.5		88	0.29	101.75	131	188	0.59	207.86
72		89	0.29	102.81	165	186	0.58	205.73
81	19	90	0.29	103.88				
95		91	0.30	104.94				
116		90	0.29	103.88				
136		89	0.29	102.81				
144		88	0.29	101.75				
155		87	0.28	100.69				
	22.5	100	0.32	114.49				
	28	110	0.35	125.10				
	34	120	0.38	135.71				
	39	125	0.40	141.01				
	44	130	0.41	146.32				
	50	135	0.43	151.62				
	56.5	140	0.44	156.93				
	62	143	0.45	160.11				
	77	150	0.47	167.54				
	80	151	0.48	168.60				
	82	152	0.48	169.66				

1	2			3			
Jaw shift (0,1 mm)	Gauge Reading	≈ Load (kN)	$\bar{\sigma}_1 - \bar{\sigma}_3$ (kPa)	Jaw shift	Gauge Reading	≈ Load (kN)	$\bar{\sigma}_1 - \bar{\sigma}_3$
	90	154	0.49	171.78			
	98.5	156	0.49	173.90			
	101	157	0.49	174.96			
	104.5	158	0.50	176.03			
	116	159	0.50	177.09			
	120	160	0.50	178.15			
	124	161	0.51	179.21			
	131	162	0.51	180.27			
	150	163	0.51	181.33			
	161	164	0.52	182.39			
	174	165	0.52	183.45			
	197	166	0.52	184.51			
Achieved 15% of axial deformation (18 mm), test ended.							

Figure 6-29. Triaxial test of 1% reinforced soil, data measured and computed

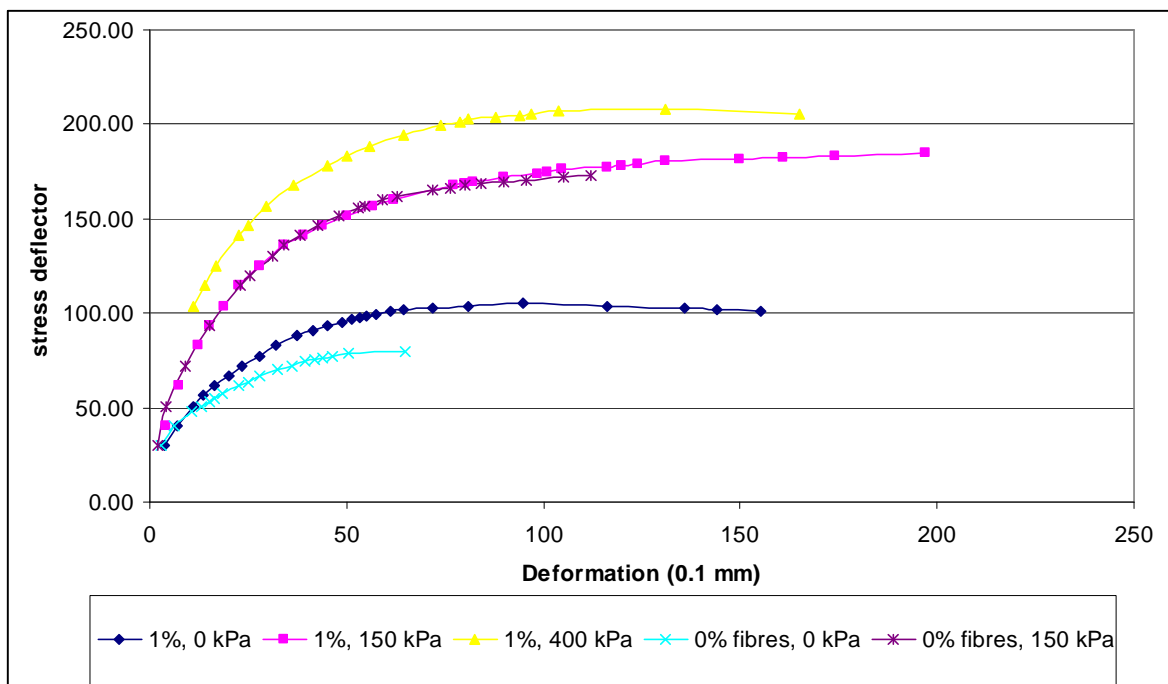


Figure 6-30. Stress-deformation curves, Test III (1% reinforcement) + unreinforced specimens

Comparison to existing laboratory results

Some laboratory results showing behaviour of soil reinforced with the fibres were accomplished by Texas Transportation Institute: Figure 6-31 and Figure 6-32 give stress-strain curves for the clay and sand, respectively. Figure 6-31 shows that addition of fibers into the stabilized clay increases the peak strength, the modulus, and the residual strength when compared with clay with only chemical stabilization. Figure 6-32 shows the same type of effect for stabilized

sand. Interestingly, Figure 6-32 also reveals that the residual strength for the sand with 5-percent portland cement and 0.5-percent fibers is significantly greater than that for the sand with 9-percent portland cement and no fibers (at larger values of strain). [3]

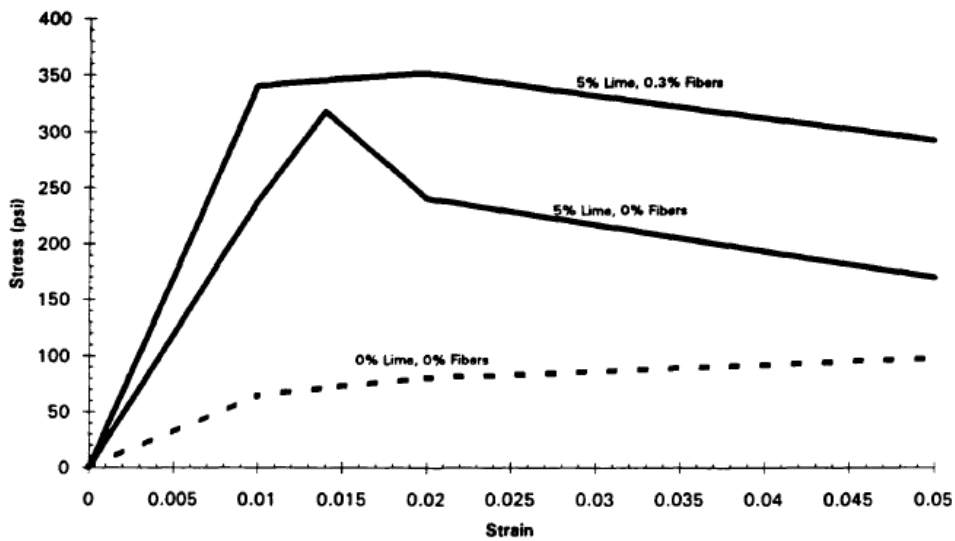


Figure 6-31. Stress-Strain Curves for Clay [3]

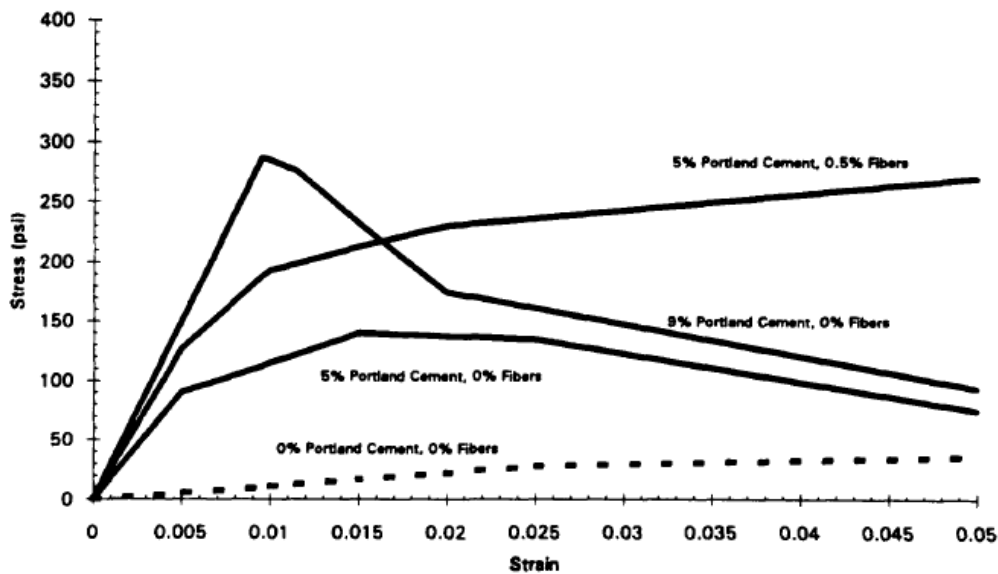


Figure 6-32. Stress-Strain Curves for Sand [3]

6.7.2.3. Evaluation by Mohr's Circle Diagram

Finally, the tests results are plotted in Mohr's circles, where stress strengths (stress deflectors), peak friction angles, shear strengths and the shear strength envelope can be read and compared. More on Mohr in chapter 4.6.

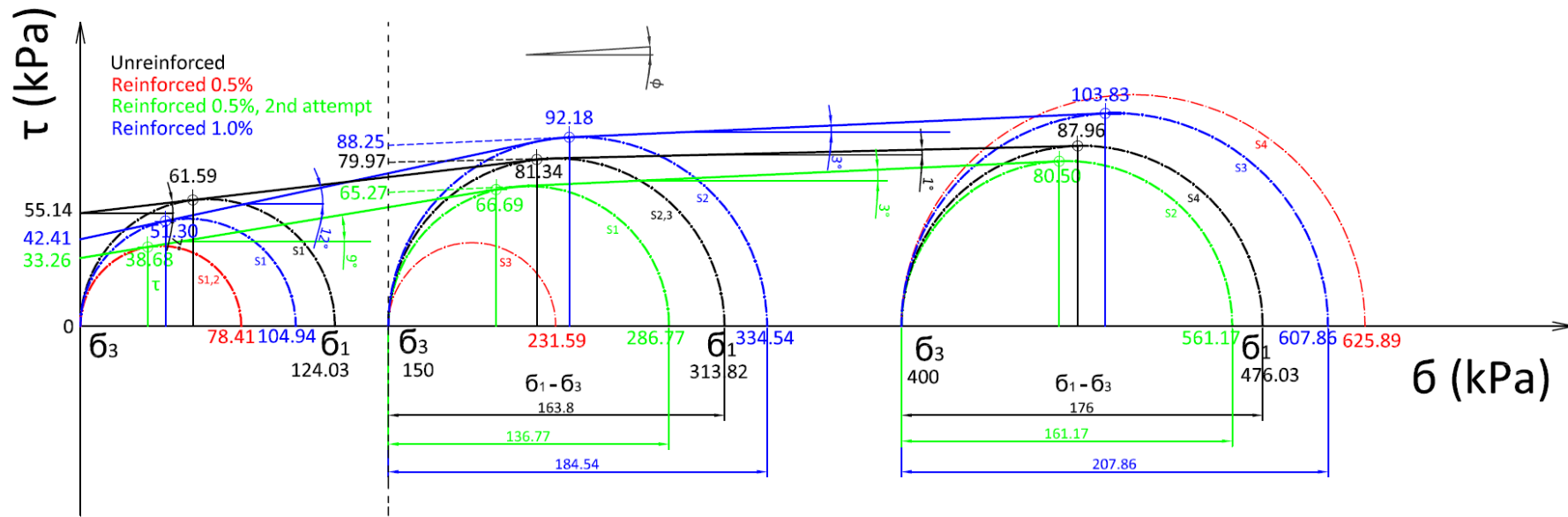


Figure 6-33. Mohr circles and shear envelope

7. Conclusion

Although the fibre-reinforcement doesn't increase the shear strength of the soil considerably, it does increase the post-peak strength. While an unreinforced clayey soil post-peak duration quickly falls down, the reinforced clayey soil exhibits either the same level of the post-peak strength as the level of the peak strength, or a very slow and gradual decrease.

These results indicate that the fibre-reinforcement can be used in practice in specific cases. It can be an alternative method of geotechnical engineering as well as e. g. soil stabilisation is. The use could be useful especially in combinations with other soil/geotechnical/construction elements, together creating a complex solution.

BIBLIOGRAPHY

- [0] Author's pictures taken in the faculty geotechnical laboratory, yr 2009.
- [1] Holtz, D. Robert. *Geosynthetics for Soil Reinforcement* [online]. Seattle, Washington, November 2001.
URL: <https://ceprofs.civil.tamu.edu/briaud/Buchanan%20Web/Lectures/Ninth%20Buchanan%20Lecture.pdf> [cit. 2009-03-18].
- [2] Zornberg, Jorge G. *Advances in Reinforced Soil Technology* [online]. Department of Civil, Architectural and Environmental Engineering, University of Texas at Austin, 2005.
URL: http://www.ce.utexas.edu/prof/zornberg/zornberg-publication_files/Zornberg/Zornberg%20nonreferreed/Zornberg_2005.pdf [cit. 2009-03-18].
- [3] Grogan, William P.; Johnson, Wayne G. *Stabilization of High Plasticity Clay and Silty Sand by Inclusion of Discrete Fibrillated Polypropylene Fibers (Fibergrids®) for Use in Pavement Subgrades*. U.S. Army Corps of Engineers, May 1994. Final Report CPAR-GL-94-2.
- [4] Li, Chunling. *Mechanical Response of Fiber-reinforced Soil* [online]. Dissertation Thesis, The University of Texas at Austin, May 2005.
URL: <https://repositories.lib.utexas.edu/bitstream/handle/2152/1781/lic25697.pdf?sequence=2>. [cit. 2009-03-18].
- [5] *Integrated Publishing* [online].
URL: http://www.tpub.com/content/engineering/14071/css/14071_389.htm [cit. 2009-05-15].
- [6] Day, Robert W. *Soil testing manual: procedures, classification data, and sampling practices*. McGraw-Hill Professional, 2001. ISBN 0071363637, 9780071363631.
- [7] *Cvičení č. 3: Stanovení zrnitosti zemin*. Department of Infrastructure: Geotechnika a zakládání staveb, Jan Perner Transport Faculty.
- [8] *Atterberg limits* [online]. Wikipedia, the free encyclopedia, last modification 2009-05-19.
URL: http://en.wikipedia.org/wiki/Atterberg_limits [cit. 2009-05-17].
- [9] *Liquid Limit: Cone Penetrometer Method* [online]. Main Roads Western Australia. Issue 1 09/87.
URL: http://www2.mainroads.wa.gov.au/NR/rdonlyres/688EAC66-D077-4500-A017-6885F869B196/0/wa120_2.pdf [cit. 2009-05-17].
- [10] *Plasticity Chart for the Unified Soil Classification System* [online]. Last modified 2006-12-19.
URL: <http://www.crma.ac.th/cedept/CourseWare/Geotech/CE4304/Chapter1/Images/PlastChart.gif> [cit. 2009-05-18].
- [11] *Unified Soil Classification System – ASTM D2488* [online]. Gint Software, last revision 2005-09-26.
URL: http://www.gintsoftware.com/downloads/reports/lgd_a_nnnn03.pdf [cit. 2009-05-18].
- [12] *Grain Size Distribution* [online]. University of Texas at Arlington, Thursday 02-05-04.

- URL: http://geotech.uta.edu/lab/Main/Soil%20Lab/03_Sieve%20analysis/Sieve%20analysis.pdf
[cit. 2009-05-20].
- [13] Geotextile [online]. Germes Online.
URL: <http://www.germes-online.com/catalog/13/701/128620/geotextile.html> [cit. 2009-05-20].
- [14] Geogrids: http://www.permathene.com/htm/photographs/photo_geogrids.shtml [cit. 2009-03-18].
- [15] Geonet: <http://www.germes-online.com/direct/dbimage/50086415/Geonet.jpg> [cit. 2009-03-18].
- [16] *Geotechnical Laboratory Experiments* [online].
URL: <http://home.iitk.ac.in/~madhav/geolab.html> [cit. 2009-05-20].
- [17] *ENCE 361 Soil Mechanics: Unconfined Compression Test* [online]. Vulcanhammer.net.
URL: <http://www.vulcanhammer.net/utc/ence361/f2001/361-II8.pdf> [cit. 2009-05-20].
- [18] *Stress-strain curve* [online]. Wikipedia, the free encyclopedia, last modified on 18 May 2009.
URL: http://en.wikipedia.org/wiki/Stress-strain_curve [cit. 2009-05-21].
- [19] Lamboj, L.; Štěpánek, Z. *Mechanika zemin a zakládání staveb*. ČVUT, 2005.
- [20] *Operating Instruction: Multiplex 50*. ELE International, 2004. 9901X0236 Issue 3.
- [21] <http://www.kern-vahy.cz/cz/partnershop/catalogue-28.html> [cit. 2009-05-22].
- [22] Newark.
URL: <http://www.newark.com/jsp/search/productdetail.jsp?sku=53M7381&requestid=275793>.
[cit. 2009-05-25].
- [23] BMT. Venticell 111 [online].
URL:
http://www.bmt.cz/goodsdetail_Is.asp?nGoodsID=1355&nDepartmentID=284&nLanguageID=2
[cit. 2009-05-25].
- [24] Šmejda, A. *Experimentální posouzení stability vyztužených zemních těles*. Dissertation work, Jan Perner Transport Faculty, University of Pardubice, August 2008.
- [25] *Cvičení č. 4: Pojmenování, popis a zatřídění zemin*. Department of Infrastructure: Geotechnika a zakládání staveb, Jan Perner Transport Faculty.